Title
Thermoregulation via Temperature-Dependent PGD_2 Production in Mouse Preoptic Area.

Journal
Neuron, 103(2)

ISSN
0896-6273

Authors
Wang, Tongfei A
Teo, Chin Fen
Åkerblom, Malin
et al.

Publication Date
2019-07-01

DOI
10.1016/j.neuron.2019.04.035

Peer reviewed

Published in final edited form as:

Neuron. 2019 July 17; 103(2): 309–322.e7. doi:10.1016/j.neuron.2019.04.035.

Thermoregulation via Temperature-dependent PGD_2 Production in Mouse Preoptic Area

Tongfei A. Wang[1], **Chin Fen Teo**[1,2], **Malin Åkerblom**[3,4], **Chao Chen**[1], **Marena Tynan-La Fontaine**[1,2], **Vanille Juliette Greiner**[3,4], **Aaron Diaz**[5], **Michael T. McManus**[3,4], **Yuh Nung Jan**[1,2], and **Lily Y. Jan**[1,2,*]

[1]Departments of Physiology, Biochemistry and Biophysics, University of California, San Francisco, CA, 94158, U.S.A

[2]Howard Hughes Medical Institute, University of California, San Francisco, CA, 94158, U.S.A

[3]Department of Microbiology and Immunology, University of California, San Francisco, CA, 94158, U.S.A

[4]UCSF Diabetes Center, University of California, San Francisco, CA, 94158, U.S.A

[5]Department of Neurological Surgery, University of California, San Francisco, CA, 94158, U.S.A

SUMMERY

Body temperature control is essential for survival. In mammals, thermoregulation is mediated by the preoptic area of anterior hypothalamus (POA), with ~30% of its neurons sensitive to brain temperature change. It is still unknown whether and how these temperature-sensitive neurons are involved in thermoregulation, because for eight decades they can only be identified via electrophysiological recording. By combining single-cell RNA-seq with whole-cell patch-clamp recordings, we identified *Ptgds* as a genetic marker for temperature-sensitive POA neurons. We then demonstrated these neruons' role in thermoregulation via chemogenetics. Given that *Ptgds* encodes the enzyme that synthesizes prostaglandin D2 (PGD_2), we further explored its role in thermoregulation. Our study revealed that rising temperature of POA alters the activity of *Ptgds*-expressing neurons so as to increase PGD_2 production. PGD_2 activates its receptor DP1 and excites downstream neurons in the ventral medial preoptic area (vMPO) that mediates body temperature decrease – a negative feedback loop for thermoregulation.

*Lead Contact: lily.jan@ucsf.edu.

AUTHOR CONTRIBUTIONS

Conceptualization and Methodology, T.A.W. and L.Y.J.; Investigation, T.A.W., C.F.T., M. Å., C. C., and M.T.F.; Software, A.D.; Resource, V.J.G.; Formal Analysis, Data Curation, and Visualization, T.A.W.; Writing - Original Draft, T.A.W. and L.Y.J.; Writing - Review & Editing, C.F.T., M. Å., C.C., M.T.F., V.J.G., A.D., M.T.M., and Y.N.J.; Supervision, Project Administration, and Funding Acquisition, M.T.M., Y.N.J. and L.Y.J.

DECLARATION OF INTERESTS

The authors declare no competing interests.

DATA AND SOFTWARE AVAILABILITY

The raw reads of the sequencing data is submitted to NCBI-GEO (GSE126657, "*Genetic markers for temperature-sensitive neurons in mouse preoptic area*").

Graphical Abstract

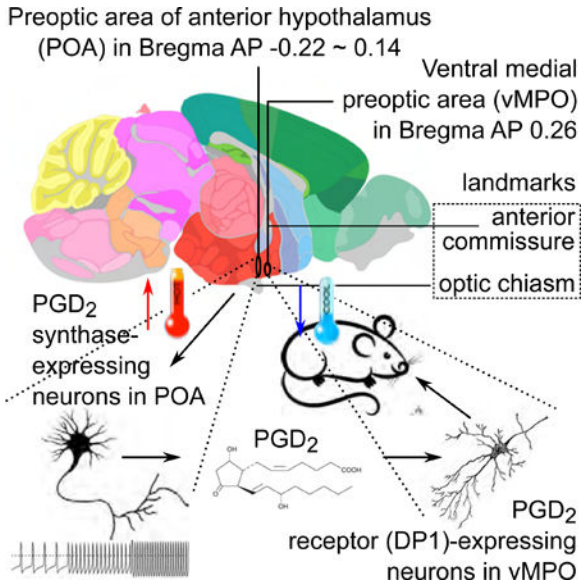

eTOC Blurb

Single-cell RNA-seq combined with whole-cell patch-clamp recording identifies PGD_2 synthase enriched in temperature-sensitive neurons in mouse medial preoptic area, which detects brain temperature increase and mediates body temperature decrease via PGD_2 receptor DP1 expressed in ventral medial preoptic area.

INTRODUCTION

It is essential for animals to maintain their core body temperature (T_c) at the optimal level. Hyperthermia or hypothermia will greatly decrease the physiological efficiency; severe deviations of the T_c could be life threatening (Gordon, 2012; Nakamura, 2011). In mammals, thermoregulation is mediated by the preoptic area of the anterior hypothalamus (POA), one of the very few brain regions that are “thermosensitive” (Boulant and Dean, 1986; Morrison, 2016). Besides ensuring a steady brain temperature during exercise, intake of hot or cold fluids, or upon prolonged exposure to extreme thermal conditions, brain temperature sensation is also important for adjusting the T_c over the circadian cycle or in response to pathogen-induced fever (Nakamura, 2011; Refinetti and Menaker, 1992). Remarkably, transgenic mice with slightly raised hypothalamic temperature exhibit a corresponding reduction of T_c, leading to an increased life span (Conti et al., 2006).

Local temperature change in the hypothalamus alters the firing rate of ~30% of neurons in medial and lateral POA, namely the temperature-sensitive neurons (Boulant and Dean, 1986; Magoun et al., 1938), and elicits thermoregulatory responses (Carlisle, 1966; Carlisle and Laudenslager, 1979; Hemingway et al., 1954). Intermingled with the temperature-sensitive neurons are temperature-insensitive neurons regulating drinking (Abbott et al., 2016), feeding (Yu et al., 2016), parental behaviors (Wu et al., 2014), and sleep (Chung et al., 2017). For eight decades, the only way to identify temperature-sensitive neurons is by

electrophysiological recording (Griffin and Boulant, 1995; Magoun et al., 1938). Identification of molecular markers for temperature-sensitive neurons will enable modern genetic-based approaches to dissect neural circuits and study the molecular mechanism underlying thermoregulation.

Central neurons known to be responsive to elevation of ambient temperature include subpopulations of neurons in the median POA (MnPO) that express leptin receptors (Yu et al., 2016), neurons in ventral MnPO and ventral medial POA (vMPO) that express BDNF and PACAP (Tan et al., 2016; Zhao et al., 2017), as well as GABAergic neurons in ventral lateral POA (vLPO)(Zhao et al., 2017). These neurons, however, do not respond to brain temperature changes (Tan et al., 2016; Yu et al., 2016; Zhao et al., 2017). One study used microarray to analyze transcripts from 8 warm-sensitive neurons in POA (Eberwine and Bartfai, 2011); however, markers of temperature-sensitive neurons could not be identified without comparison with the transcriptomes of temperature-insensitive neurons. Another study found TRPM2 to be essential for temperature sensation of POA (Song et al., 2016). While TRPM2 likely contributes to the detection of heat stress and the resulting modulation of T_c during fever, its expression is not limited to temperature-sensitive neurons (Song et al., 2016).

In light of the paucity of genetic tools that specifically target temperature-sensitive neurons, we began our study searching for molecular markers of temperature-sensitive neurons by combining RNA sequencing at the single-cell level (single-cell RNA-seq) (Poulin et al., 2016) with whole-cell patch-clamp recordings(Cadwell et al., 2016; Fuzik et al., 2016), for examination of the transcriptome of each neuron in the context of its physiological function. One marker gene of temperature-sensitive neurons identified in this study is *Ptgds*, leading us to test for its contribution to thermoregulation.

The gene *Ptgds* encodes lipocalin-type prostaglandin-D synthase (L-PGDS) that generates prostaglandin D2 (PGD_2) (Smith et al., 2011). PGD_2 is a lipid hormone best known for its involvement in reproduction (Rossitto et al., 2015). In the brain, it serves as a neuromodulator that facilitates homeostatic regulation of a variety of physiological processes including sleep (Matsumura et al., 1994) and feeding (Ohinata et al., 2008). PGD_2 usually functions in a manner antagonistic to its isomer, prostaglandin E2 (PGE_2) (Saper et al., 2012), which participates in the neuromodulation of wakefulness (Onoe et al., 1992) and anorexia (Ohinata et al., 2006). PGE_2 has been well characterized as the hormone that mediates body temperature elevation (fever) in response to pathogen-induced inflammation (Lazarus et al., 2007; Ushikubi et al., 1998). Notwithstanding the hypothermia induced by exogenous PGD_2 injected into the cerebral ventricle of the rat (Ueno et al., 1982), whether and how endogenous PGD_2 might be involved in thermoregulation remains an outstanding question (Romanovsky and Garami, 2010).

In this study, we identified the temperature-sensitive POA neurons as the endogenous source of PGD_2 for thermoregulation; the enriched expression of L-PGDS in temperature-sensitive POA neurons can be used a molecular marker to further dissect the neural circuit of thermoregulation.

RESULTS

Genetic and functional profiling of POA neurons via single-cell RNA-seq combined with whole-cell patch-clamp recording

To search for molecular markers of temperature-sensitive neurons in medial and lateral POA, we performed whole-cell patch-clamp recordings in freshly prepared mouse brain slices, followed by single-cell RNA-seq of 68 neurons (Figures 1, S1, and S2). Current-clamp recordings of neurons with spontaneous action potential (SAP) firing at different temperatures (33°C, 36°C, and 39°C) identified warm-sensitive neurons (Figures 1C and 1F, $N = 18$, SAP frequency change per degree of temperature change (dF/dT) > +0.8 Hz/°C), cold-sensitive neurons (Figures 1D and 1G, $N = 4$, dF/dT < −0.6 Hz/°C), and temperature-insensitive neurons (Figures 1E and 1H, $N = 24$, −0.6 Hz/°C < dF/dT < +0.8 Hz/°C), with electrophysiological properties consistent with previous reports (Boulant and Dean, 1986; Griffin and Boulant, 1995). In addition, we found two sub-types of silent neurons that did not fire SAP throughout the recording, including 12 “temperature-insensitive silent neurons” that exhibited very stable membrane potential (V_m), input resistance (R_{in}), time constant (τ), and spontaneous post-synaptic potentials at low frequency regardless of the temperature changes (Figures 1I and S1), and 10 “temperature-sensitive silent neurons” that exhibited temperature-dependent and reversible changes in V_m, R_{in}, τ, and noticeable high frequency spontaneous synaptic potentials during temperature rising (Figures 1J and S1).

Immediately following electrophysiological recordings, each neuron was harvested individually to generate single-cell cDNA libraries via SMART-Seq2 (Picelli et al., 2013, 2014). Detailed protocols and quality control (QC) criteria are described in STAR Methods and Supplemental Information (Figure S2). Neurons with characterized responses to temperature changes were classified by K-means clustering, based on the principal component analysis (PCA) of their gene expression profiles (Figure 1K, 4 groups, 5 replicates), and color-labeled based on temperature sensitivity (Figure 1L). Notably, in K-means clustering (Figure 1K), the left two clusters are mainly temperature-sensitive (colored in red and white in Figure 1L), while the right two clusters are mainly temperature-insensitive (colored in green and black in Figure 1L). These results imply the classification of POA neurons as in Figure 1P, based upon both their transcription profiles and temperature sensitivity. Since the algorithm dictated to remove genes expressed in fewer than 10% of the libraries, it was impossible to identify potential marker genes specifically expressed in the 4 cold-sensitive neurons.

Identification of *Ptgds* as a marker for temperature-sensitive POA neurons

To identify marker genes for temperature-sensitive neurons, we examined the expression of genes ($N = 9949$) via PCA (Figures 1M and S3B). We focused on *Ptgds* as a candidate marker and used *Camk1* for comparison and contrast. The expression ratio of these two genes (at the cDNA level, quantified in log-scaled counts per million reads, $\log_2$CPM) in different sub-populations of neurons in POA was plotted in Figure 1N. The protein products of *Ptgds* and *Camk1* were further examined by immunostaining (Figure 1O, 3 replicates), revealing non-overlapping expressions in two separate neuronal populations. Consistent with the outcome of PCA, differential expression (DE) analysis revealed that the expression level

of *Ptgds* in temperature-sensitive neurons is significantly higher than that in temperature–insensitive neurons (Figure S3A and Table S1, FDR < 0.05).

To validate *Ptgds* as a marker gene for temperature-sensitive POA neurons, we imported the $Ptgds^{tm1.1(cre)Gvn}$ (PGDS-Cre) transgenic mice that express the Cre recombinase in *Ptgds*-expressing cells (Kalamarides et al., 2011), and crossed them with the B6;129S6-*Gt(ROSA)26Sor*$^{tm14(CAG-tdTomato)Hze}$/J (Ai14) mice for Cre driven tdTomato expression. Immunostaining of L-PGDS, CaMKI, and tdTomato in POA slices from PGDS-Cre/Ai14 mice revealed co-localization of tdTomato with L-PGDS but not CaMKI (Figures 2A, 2B, and S3C, 3 replicates). We further examined the temperature-sensitivity of neurons with or without PGDS-Cre driven tdTomato expression (Figures 2C and 2D), and found that the majority of neurons without tdTomato were temperature-insensitive (17 of 20 recorded neurons, tdTomato-/normal ACSF, $P < 0.01$, Chi-square test as compared to 36 of 68 recorded neurons from WT mice), while the majority of neurons with tdTomato expression were temperature-sensitive (17 of 20 recorded neurons, tdTomato+/normal ACSF, $P < 0.01$, Chi-square test as compared to 32 of 68 recorded neurons from WT mice). Furthermore, blocking glutamate- and GABA-mediated synaptic transmission with inhibitors of AMPA-receptors (DNQX, 20 μM), NMDA-receptors (AP5, 50 μM), and $GABA_A$-receptors (SR 95531, 20 μM) resulted in the elimination of cold-sensitive neurons and temperature-sensitive silent neurons (tdTomato+/synaptic transmission blocked, $P < 0.05$, Chi-square test as compared to tdTomato+/normal ACSF), consistent with previous studies showing that perturbing synaptic transmission via reduction of extracellular Ca^{2+} level abolishes cold-sensitive POA neurons (Kelso and Boulant, 1982).

Involvement of *Ptgds*-expressing POA neurons in thermoregulation

To test for the role of temperature-sensitive POA neurons in thermoregulation, we monitored T_c of the mice with implanted temperature probe while altering action potential firing of *Ptgds*-expressing POA neurons via engineered G-protein coupled receptors known as Designer Receptors Exclusively Activated by Designer Drugs (DREADD), hM3Dq and hM4Di (Krashes et al., 2011). Upon binding to the ligand clozapine (Gomez et al., 2017), hM3Dq enhances neuronal firing of *Ptgds*-expressing neurons in a manner that mimicked the effect of temperature elevation of brain slices with warm-sensitive neurons (Figures 3A and S4E, $N = 10$, $P < 0.01$, paired Student's T-test); in contrast, clozapine silenced *Ptgds*-expressing neurons with hM4Di expression (Figures 3G and S4E, $N = 10$, $P < 0.01$, paired student's T-test) thereby simulating the response of warm-sensitive neurons to brain temperature reduction. *Ptgds*-expressing neurons with mCherry expression only were not responsive to clozapine treatment (Figure S4E, $N = 10$, $P > 0.05$, paired student's T-test).

Since the T_c oscillates with circadian rhythm over a period of 24 hours, we administered clozapine at different zeitgeber times (ZT) in the same mouse. Animals with hM3Dq expression in *Ptgds*-expressing POA neurons exhibited a significant reduction in T_c as compared to vehicle control, in response to clozapine IP injection at the beginning of nighttime when T_c is normally high (Figures 3B, 3C, and 3E, $N = 8$, $P < 0.05$ at 1–2 hour following IP, paired Student's T-test), but they displayed no significant alteration of T_c with clozapine IP injection in early daytime when T_c is normally low (Figures 3B, 3D, and 3F, *N*

= 8, P > 0.05, paired Student's T-test). In contrast, the T_c of mice with hM4Di expression in *Ptgds*-expressing POA neurons was higher with clozapine treatment than vehicle control, for IP injection in early daytime (Figures 3H, 3I, and 3K, N = 7, P < 0.01 at 1–2 hour following IP, paired Student's T-test) but not for IP injection in early nighttime (Figures 3H, 3J, and 3L, N = 7, P > 0.05, paired Student's T-test). Control mice with Cre-dependent mCherry expression in POA displayed no alteration of T_c following clozapine IP injection (Figure S4D, N = 7, P > 0.05, paired Student's T-test). These results demonstrate that the *Ptgds*-expressing POA neurons, which are mainly temperature-sensitive, are involved in body temperature control in accordance with circadian oscillation.

Temperature-dependent PGD_2 production in POA

To explore the potential role of L-PGDS in thermoregulation, we first examined the amount of its enzymatic product, PGD_2, as a function of temperature. Following incubation of the brain slice (trimmed to exclude brain regions other than POA) at a specified temperature (33°C, 36°C, or 39°C), we employed liquid chromatography–tandem mass spectrometry (LC-MS/MS) in the multiple reaction monitoring (MRM) mode to measure PGD_2 and PGE_2 extracted from the brain slice (Figure 4A) (Farias et al., 2008).

Whereas no differences were detectable with 5 min incubation at various temperatures (Figure 4B, N = 6, P > 0.05, One-way ANOVA), a greater amount of PGD_2 was detected with 30 min incubation at 39°C than those at 36°C or 33°C (Figure 4C, N = 6, P < 0.01, One-way ANOVA followed by Tukey's multiple comparisons test). In contrast, brain slices of the thalamus mainly composed of temperature-insensitive neurons but with L-PGDS expression level comparable to that of POA (Figure S5), displayed no difference in PGD_2 production at different temperatures (Figure 4D, N = 6, P > 0.05, One-way ANOVA). Hence the temperature dependent PGD_2 production in POA cannot be attributed to the temperature coefficient (Q10) of PGDS enzyme activity.

Blockade of action potential firing by TTX (1 μM) or removal of extracellular Ca^{2+} (Ca^{2+}-free ACSF with 10 mM EGTA) during the 30 min incubation abolished the temperature-dependent PGD_2 production in POA slices (Figures 4E and 4F, N = 6, P > 0.05, One-way ANOVA) and caused the overall PGD_2 production to drop below that in the normal condition of 36°C/30-min (compared to Figure 4C, N = 6, P < 0.01, One-way ANOVA followed by Tukey's multiple comparisons test), likely reflecting a Ca^{2+} dependence of PGDS enzyme activity (Irikura et al., 2009). Whereas blocking synaptic transmission eliminated the cold-sensitive and temperature-sensitive silent neurons in POA (Figure 2D), it did not eliminate temperature-dependent PGD_2 production (Figure 4G, N = 6, P < 0.01, One-way ANOVA followed by Tukey's multiple comparisons test).

Consistent with the notion that PGE_2 is produced in the periphery rather than the central nervous system (Ivanov and Romanovsky, 2004), the PGE_2 levels in POA were much lower than the PGD_2 levels, and exhibited no significant variation with temperature (Figures 4B–4G, red, N = 6, P > 0.05, One-way ANOVA).

PGD_2 provides protection during hyperthermia by mediating T_c decrease

To study the physiological role of endogenous PGD_2 in thermoregulation, we inhibited L-PGDS with AT-56 (Irikura et al., 2009). LC-MS/MS analysis confirmed that AT-56 (20 μM, incubated in 39°C for 30 min) diminished newly-synthesized PGD_2 in POA slices (Figure 5A, $N = 6$, $P < 0.05$, Student's T-test). Having found that IP injection of AT-56 (20 mg/kg body weight) did not alter the T_c of mice at room temperature in midday (Figures 5B and 5C, black and green, $N = 6$, $P > 0.05$, One-way ANOVA), we tested for its effect in a fever model of hyperthermia induced by intracerebroventricular (ICV) injection of PGE_2 (Ushikubi et al., 1998). IP injection of AT-56 caused mice to respond to ICV injection of PGE_2 (2 nmol in 1 μl) with a greater increase in T_c as compared to mice with IP injection of vehicle control (Figures 5B and 5C, red and blue, $N = 6$, $P < 0.01$, One-way ANOVA followed by Tukey's multiple comparisons test).

We next studied the effect of exogenously introduced PGD_2 in thermoregulation. ICV injection of PGD_2 (2 nmol in 1 μl) led to hypothermia in mice (Figures 5D and 5E, $N = 6$, $P < 0.01$, One-Way ANOVA with repeated measurement, followed by Sidak's multiple comparisons test), consistent with previous reports in rat (Ueno et al., 1982). Simultaneous T_c recording and movement tracking revealed comparable levels of locomotor activities of mice injected with PGD_2 or vehicle control (Figures 5F–5H, $P > 0.05$, One-Way ANOVA with repeated measurement, followed by Sidak's multiple comparisons test), indicating that the effect of PGD_2 in reducing T_c cannot be attributed to potential side effects on locomotor activities.

PGD_2 excites neurons in the ventral medial preoptic area (vMPO) by activating the PGD_2 receptor DP1

To explore the underlying mechanism of PGD_2-induced hypothermia, we looked for PGD_2 receptors in brain regions that are involved in thermoregulation. Of the two endogenous PGD_2 receptors, DP1 is primarily associated with PGD_2 function in the brain (Saper et al., 2012; Woodward et al., 2011). Having found that IP injection of the DP1 inhibitor, MK-0524 (4 mg/kg body weight) (Cheng et al., 2006), abolished the PGD_2-induced hypothermia (Figures 5D and 5E, $N = 6$, $P > 0.05$, One-Way ANOVA with repeated measurement), we performed immunostaining and localized DP1 expression in the vMPO (Figures 6B and S6C, 3 replicates). Given that the vMPO neurons expressing BDNF and PACAP mediate T_c decrease in response to ambient temperature elevation (Tan et al., 2016; Zhao et al., 2017), it is notable that the distribution of DP1 overlapped with that of BDNF in the putative soma of vMPO neurons, and with that of PACAP in putative neuronal processes along the 3rd ventricle (Figures 6B, S6C and S6E). In contrast, there was limited expression of DP1, BDNF, and PACAP in the medial and lateral POA that is located ~100 μm posterior from vMPO (Figures S6D and S6F).

These findings prompted the intriguing hypothesis that PGD_2 released from POA induces hypothermia by activating the DP1-expressing vMPO neurons (Figure 6A and graphical abstract). To look into this possibility, we first examined the response of vMPO neurons to PGD_2 applied at the location corresponding to the bottom of the 3rd ventricle (Figure 6C). Whereas vMPO neurons were silent or exhibited low frequency SAP at rest, these neurons

increased their firing rate following a puff application of PGD_2 (20 μM, ~10 s, Figures 6D and 6E, red, $N = 7$, $P < 0.01$, paired Student's T-test), but not in the presence of the DP1-inhibitor MK-0524 (100 nM during the entire episode of recording) (Figures 6D and 6E, blue, $N = 7$, $P > 0.05$, paired Student's T-test).

Next, we employed optogenetics to test whether PGDS-expressing POA neurons release PGD_2 to modulate vMPO neuronal activity. AAV constructs of Cre-dependent ChR2 were injected into medial and lateral POA of mice expressing PGDS-Cre, followed by recording from vMPO neurons 2–3 weeks after the viral injection (Figure 6F). Laser activation (30 s) of ChR2 in axons of POA neurons expressing PGDS-Cre enhanced the neuronal firing in vMPO neurons in the presence of blockers of AMPA-receptors (DNQX, 20 μM), NMDA-receptors (AP5, 50 μM), and $GABA_A$-receptors (SR 95531, 20 μM) (Figures 6G and 6H, $N = 24$, $P < 0.01$, One-Way ANOVA with repeated measurement, followed by Sidak's multiple comparisons test). This excitatory effect was abolished by inhibiting the PGD_2 receptor DP1 (MK-0524, 100 nM, Figures 6G and 6H, $N = 18$, $P > 0.05$, One-Way ANOVA with repeated measurement). No alteration of neuronal firing was detected with laser illumination of brain slices from mice injected with control AAV constructs of Cre-dependent mCherry (Figure S7, $N = 18$, $P > 0.05$, One-Way ANOVA with repeated measurement). These results reveal that PGDS-expressing neurons in POA project to vMPO and release PGD_2 to excite vMPO neurons.

The PGD_2 synthase (L-PGDS) in the POA is essential for the homeostasis of thermoregulation

To test whether *Ptgds* expression in POA is essential for homeostatic thermoregulation, we employed CRISPRi to knock down *Ptgds* specifically in the POA. Lentivirus constructs of sgRNA-*Ptgds* or negative control (NT, non-targeting) were injected into medial and lateral POA of mice with constitutive expression of dCas9-KRAB, and the mouse T_c was recorded with an implanted temperature probe (Figure 7A). In contrast to the viability and normal T_c (with circadian oscillation) of mice injected with the control virus, mice with *Ptgds* knockdown in POA could no longer hold their body temperature three weeks following viral injection, and died soon afterwards (Figures 7E–7G, $N = 6$ in each group, $P < 0.01$, log-rank test). Periodogram analysis of T_c oscillation 13–17 days following viral injection revealed dampened amplitude and shortened period in mice with *Ptgds* knockdown (Figures 7H and 7I, $N = 6$ in each group, $P < 0.05$, Student's T-test), while the midline T_c and phase of peak T_c remained unaltered (Figures 7J and 7K, $N = 6$ in each group, $P > 0.05$, Student's T-test). Antibody staining of L-PGDS and GFP, a reporter for viral transfection and construct expression, in POA slices indicated that ~60% reduction of *Ptgds* expression in medial and lateral POA (Figures 7B–7D, $N = 3$ in each group, $P < 0.01$, Student's T-test) causes lethality (Figure 7G).

By challenging virally injected mice of a separated cohort with elevated ambient temperature at 37°C (for 4 hours) 2 weeks following the lentivirus injection, we found that mice with *Ptgds* knockdown in the POA displayed a greater elevation of T_c than those with control vector injection (Figures 7L and 7M, $N = 8$ for NT, $N = 9$ for *Ptgds*, $P < 0.01$, Student's T-test). Thus, L-PGDS expressed in temperature-sensitive POA neurons plays an

important role in protecting animals from hyperthermia, and its function is crucial for maintaining body temperature and survival.

DISCUSSION

A general platform to dissect neural circuits with transcriptome analyses of functionally characterized neurons

This study was initiated from an unbiased single-cell RNA-seq screening of medial and lateral POA neurons following their functional analysis via patch-clamp recording. Since Kriegstein and colleagues demonstrated experimentally that low coverage single-cell RNA-seq can reveal cellular heterogeneity in the brain (Pollen et al., 2014), high throughput sequencing with low coverage has been widely applied to dissect neural circuits (Poulin et al., 2016), including the POA (Moffitt et al., 2018). Whereas theoretical analysis predicts that a small number of samples (< 100) with high quality libraries could also allow a robust readout of the transcriptional program (Heimberg et al., 2016), there may have been some reluctance to apply this cutting-edge technology when the samples of interest are precious. Our study demonstrates that low-throughput sequencing of datasets with functional relevance is instrumental in making significant discovery. Future studies combining single-cell RNA-seq with functional characterizations such as patch-clamp recording, real-time imaging, circuit tracing, or optogenetic manipulation, could be a powerful strategy for mechanistic analyses of neural circuits with heterogeneous neuronal populations.

A genetic marker for temperature-sensitive POA neurons

The phenomenon of brain temperature sensation was first reported 80 years ago (Magoun et al., 1938), and validated in different species (Boulant and Dean, 1986). The hypothesis that temperature-sensitive POA neurons play a pivotal role in thermoregulation remained unverified for decades, until we identified the genetic marker, *Ptgds*, for temperature-sensitive POA neurons (Figures 1 and 2). In addition to allowing for manipulation of the action potential firing of the temperature-sensitive POA neurons via either chemogenetics to test how these neurons may regulate body temperature (Figure 3) or optogenetics to identify their downstream neurons in the vMPO (Figure 6), this genetic marker for temperature-sensitive neurons will greatly facilitate future research in thermoregulation.

A PGD_2-mediated negative-feedback loop for thermoregulation

Although it has been known for decades that ICV injection of PGD_2 is able to induce hypothermia in rat (Ueno et al., 1982), whether endogenous PGD_2 plays a role in regulating T_c has remained an open question. In our study, we identified the temperature-sensitive POA neurons as the endogenous source of PGD_2, with its production increased in response to rising temperature of POA brain slice. We further showed that these neurons release PGD_2 to activate the DP1-expressing neurons in vMPO, which likely correspond to a subset of the vMPO neurons that express BDNF and PACAP and mediate T_c decrease in response to ambient temperature elevation (Tan et al., 2016; Zhao et al., 2017). Our study thus uncovers a convergence of POA neurons sensitive to local hypothalamic temperature increase and neuronal pathways relaying ambient temperature increase, to activate the vMPO neurons that mediate T_c decrease, for negative feedback in the homeostasis of thermoregulation.

The expression of *Ptgds* in POA neurons

By conducting single-cell RNA-seq analysis, we found that *Ptgds* is highly expressed in temperature-sensitive POA neurons, although a much lower level of *Ptgds* transcripts was also detected in temperature-insensitive POA neurons (Figure 1N and Table S1). Importantly, immunostaining of L-PGDS and the use of the PGDS-Cre/Ai14 mouse line that labels *Ptgds*-expressing neurons with tdTomato revealed that L-PGDS is predominantly expressed in temperature-sensitive POA neurons (Figures 1O, 2A, and 2B). It is possible that the sensitivity afforded by RNA-seq is greater than that of the immunostaining. Alternatively, there could be some as yet uncharacterized mechanism that prevents *Ptgds* mRNA translation in temperature-insensitive POA neurons.

The temperature-sensitive POA neurons with high *Ptgds* expression levels are composed of three subtypes: warm-sensitive neurons, cold-sensitive neurons, and temperature-sensitive silent neurons (Figure 1P). It is possible to explore in future studies the genetic markers for different subtypes of temperature-sensitive POA neurons by employing single-cell RNA-seq (or qPCR) combined with more efficient electrophysiological recordings from *Ptgds*-expressing POA neurons that are fluorescently labeled in PGDS-Cre/Ai14 mice. In addition, this strategy might also be employed to identify channels or receptors that contribute to temperature sensation.

The function of L-PGDS in POA neurons for thermoregulation

While the initial screen identified several candidate marker genes for either temperature-sensitive neurons or temperature-insensitive neurons (Figures S3A and S3B, and Table S1), we focused on *Ptgds* mainly for the expectation that the gene product L-PGDS is functionally involved in thermoregulation.

Our study revealed that L-PGDS is directly associated with homeostasis of thermoregulation, by producing more PGD_2 in response to temperature elevation of the POA, thereby lowering the T_c. While L-PGDS is expressed not only in warm-sensitive neurons but also in cold-sensitive neurons and temperature-sensitive silent neurons, we hypothesize that in the scenario of hyperthermia (~36°C and above), warm-sensitive neurons contribute mostly to the temperature-dependent PGD_2 production and mediate body temperature decrease, for three reasons: 1) there are many more warm-sensitive neurons than cold-sensitive neurons (Figure 2D); 2) in the temperature range of 36°C – 39°C, cold-sensitive neurons as well as temperature-sensitive silent neurons are mostly silent (Figure 1G), hence they are unlikely to contribute much to PGD_2 production given its dependence on action potential firing (Figure 4E); 3) blocking synaptic transmission to mask the cold-sensitive neurons and temperature-sensitive silent neurons did not eliminate the temperature-dependent PGD_2 production (Figures 2D and 4G).

Brain region-specific knockdown of *Ptgds* via injection of the lentiviral CRISPRi construct into POA caused alteration of T_c over circadian cycle within 3 weeks of the viral injection, followed by a precipitous drop of body temperature and increasingly pronounced circadian swings, leading to death shortly thereafter (Figure 7). Removal of PGD_2 signaling by either genetic or pharmacological approach does not influence the baseline T_c (Figures 5B, 5C,

and 7K), but the malfunction can be detected upon exposure to conditions that induce hyperthermia (Figures 5B, 5C, 7L and 7M). Such a sophisticated neural circuit for thermoregulation may conceivably have been selected for in evolution, and warrants further investigation.

Differences between vMPO neurons sensitive to ambient temperature and POA neurons sensitive to brain temperature

Previous studies have examined neurons in MnPO, vMPO, and vLPO that respond to ambient temperature change (increase only). Increasing action potential firing of these neurons could lead to a decrease in T_c by up to 2°C within 20 min of neuronal activation via optogenetics (Tan et al., 2016; Zhao et al., 2017), or within 60 min of neuronal activation via chemogenetics (Yu et al., 2016). In our study, we examined a distinct population of medial and lateral POA neurons that are sensitive to temperature change (both increase and decrease) of the preoptic area. Chemogenetic manipulation of *Ptgds*-expressing POA neuronal firing at certain ZT leads to a mild (~1°C) and sustained (1~2 h) change in T_c (Figure 3). Notably, this amplitude is comparable to the amplitude of circadian oscillation of T_c in mice (Figure 7H).

The ambient temperature change usually requires immediate and robust response from the thermal effector, because the environmental condition could be harsh (sudden exposure to hot or cold environment), invoking fight-or-flight response. In contrast, the brain temperature is much more stable than the ambient temperature. The most common scenario of brain temperature change corresponds to the rhythmic oscillation over the circadian cycle (~24 h). It is a relatively slow process, and the amplitude swing is mild. So the brain temperature sensor is not prepared to, and should not be able to, induce sudden and large changes of T_c.

Circadian oscillation of T_c and the possible involvement of temperature-sensitive POA neurons

This study revealed that the temperature-dependent neuronal firing and PGD_2 production in POA is cell-autonomous, independent of synaptic transmission (Figures 2D and 4G). This finding suggests that the temperature-sensitive neurons with the signaling molecule PGD_2 are situated upstream in the circuit for thermoregulation: they receive modulatory rather than commanding input for body temperature control. One possible modulatory input is from the suprachiasmatic nucleus (SCN), the central circadian clock, in anterior hypothalamus. The circadian oscillation of T_c (Figures 3B, 3H, and 7E) has been attributed to either rhythmic synaptic input from the central circadian clock (SCN) to the thermoregulation center (POA), or hormone-like diffusible signaling from SCN to organs mediating heat loss/production that may then be modulated by the thermoregulatory system to minimize the circadian amplitude (Refinetti and Menaker, 1992). Our finding that *Ptgds* knockdown in POA dampened the amplitude of T_c oscillation over circadian cycle (Figure 7H) lends indirect support for the former scenario. Whereas projection from SCN to POA has been implicated in sleep modulation (Deurveilher and Semba, 2005), it will be interesting to test if this projection contributes to the circadian oscillation of T_c in future research.

STAR Methods

CONTACT FOR REAGENT AND RESOURCE SHARING

Further information and requests for resources and reagents should be directed to and will be fulfilled by the Lead Contact, Lily Y. Jan, lily.jan@ucsf.edu.

EXPERIMENTAL MODEL AND SUBJECT DETAILS

C57BL/6N (B6) wildtype (WT) mice used in this research were originally purchased from Charles River, San Diego, CA and bred in our colony at University of California, San Francisco. Transgenic mouse line FVB.Cg-Ptgds<tm1(cre)Gvn>/GvnRbrc (PGDS-Cre, MGI:5051626)(Kalamarides et al., 2011) was imported from RIKEN BRC, Japan, and crossed with the reporter line B6;129S6-Gt(ROSA)26Sor$^{tm14(CAG-tdTomato)Hze}$/J (Ai14, MGI:3809524) from the Jackson Lab (Bar Harbor, ME).

The dCas9-KRAB mice were generated in the FVB background with the TARGATT™ site-specific knock-in technology (Tasic et al., 2011) by introducing into the Hipp11 locus a construct with the CAG promotor driving expression of puromycin resistance, mCherry, and the dead Cas9 (dCas9) protein fused to the Krüppel Associated Box (KRAB) domain. The dCas9-KRAB protein lacks endonuclease activity but retains its ability to bind to single guide RNAs (sgRNAs) for specific gene targeting and silencing through heterochromatin formation induced by the KRAB domain (Greiner *et al.*, in preparation).

All mice were maintained under a 12:12 hour L/D schedule, and allowed to receive food and water ad libitum. Male mice at the age of 2–3 months were used in all the experiments. All protocols were approved by the IACUC at University of California, San Francisco, in full compliance with NIH guidelines for humane treatment of animals.

METHOD DETAILS

Stereotactic Injection—The pAAV-hSyn-DIO-hM3D(Gq)-mCherry, pAAV-hSyn-DIO-hM4D(Gi)-mCherry, and pAAV-hSyn-DIO-mCherry, were gifts from Bryan Roth (Addgene viral prep # 44361-AAV8, # 44362-AAV8, and # 50459-AAV8)(Krashes et al., 2011). The pAAV-EF1a-double floxed-hChR2(H134R)-mCherry-WPRE-HGHpA was a gift from Karl Deisseroth (Addgene viral prep # 20297-AAV8). PGDS-Cre mice were injected with 0.5 μl vectors at stereotactic coordinates (bilateral) of AP 0.1, ML ±0.3, DV 5.5, and allowed to recover for at least 1 week before the next experimental procedure.

Brain slice preparation—Brain slices were usually prepared 3–5 hours after light-on in the animal colony (CT 3–5). Coronal brain slices containing the preoptic area of the anterior hypothalamus (POA), the ventral medial preoptic area (vMPO), cortex, or striatum, or horizontal slices containing thalamus or hippocamus, were sectioned in chilled slicing solution (2.5 mM KCl, 0.5 mM $CaCl_2$, 10.0 mM $MgSO_4$, 1.2 mM NaH_2PO_4, 26.0 mM $NaHCO_3$, 11.0 mM glucose, and 234.0 mM sucrose, saturated with 95% O_2/5% CO_2). 300-μm-thick brain slices were sectioned using a vibrating blade microtome (Leica, Wetzlar, DE). Brain slices were trimmed to remove irrelevant brain regions, and allowed to recover in slicing solution at 35°C for 10 min, before transferring to a holding chamber containing

artificial cerebrospinal fluid (ACSF, 126.0 mM NaCl, 2.5 mM KCl, 2.5 mM $CaCl_2$, 1.3 mM $MgSO_4$, 1.2 mM NaH_2PO_4, 10.0 mM glucose, 26.0 mM $NaHCO_3$, saturated with 95% O_2/5% CO_2). Brain slices were incubated at room temperature for at least 1.5 h before electrophysiological recording or biochemistry assay.

Electrophysiology—Whole-cell patch electrodes, with pipette tip resistance of 6–10 MΩ, were filled with internal solution containing 122.0 mM K-gluconate, 13.0 mM KCl, 0.06 mM $CaCl_2$, 1.0 mM $MgCl_2$, 0.1 mM EGTA, 10.0 mM HEPES, 4.0 mM Na-ATP, and 0.4 mM Na-GTP, with pH 7.3 and osmolality 290–300 mOsm/L. For samples subjected to single-cell RNA-seq analysis, 0.1 U/μl SUPERaseIN (Thermo Fisher, South San Francisco, CA) was included. Recordings were performed using a Multiclamp 700B amplifier (Molecular Devices, Sunnyvale, CA). Signals were sampled at 10 kHz using a Digidata 1440 digitizer (Molecular Devices, Sunnyvale, CA), and stored in computer for subsequent analyses using pClamp software (Molecular Devices, Sunnyvale, CA).

The temperature in the recording chamber was controlled by an inline heater (Warner Instruments, Hamden, CT) with continuous perfusion of fresh ACSF to the recording chamber. Real-time bath temperature was recorded with a thermistor (Warner Instruments, Hamden, CT) next to the brain slice, with analog input signal processed with Digidata 1440 digitizer simultaneously as the electrophysiological recordings. Recording pipette was grounded in a separate chamber with 3 M KCl at room temperature, connected to the recording chamber by a salt bridge. Liquid junction potential was measured following the procedure in the literature (Griffin and Boulant, 1995).

Recordings were performed at CT 5–10, with each episode of recording from one neuron lasting for up to 10 min. Only one neuron was recorded and collected from a single slice. Upon break-through, the neuron was first subjected to a current-steps protocol from −100 pA to +100 pA (20 pA interval) at 36°C, so as to measure the basic membrane properties. The neuron was then recorded under current-clamp, 15 sec per sweep, with a −20 pA/20 ms current injection in each sweep, to monitor the membrane properties. In addition to the electrophysiological recordings, the location of the recorded neuron in the brain slice was captured by CCD camera, and further measured in terms of the distances to the third ventricle (x) and optic chiasm (y) as in Figure 1B.

To characterize the temperature sensitivity of a neuron, the bath temperature of the recording chamber was adjusted from 36°C to 33°C, then to 39°C, and then back to 36°C (2–3 min at each temperature). More than 96 neurons were recorded from POA slices of WT mice and harvested for single-cell RNA-seq; 60 neurons were recorded from POA slices of PGDS-Cre/Ai14 mice, including 20 neurons without tdTomato expression (*Ptgds*-), 20 neurons with tdTomato expression (*Ptgds*+), and 20 neurons labeled with tdTomato (*Ptgds*+) and recorded in ACSF containing DNQX (20 μM), AP5 (50 μM), and SR 95531 (20 μM) (all from Tocris, Bristol, UK).

To validate the effect of Designer Receptors Exclusively Activated by Designer Drugs (DREADD) on neuronal firing of *Ptgds*-expressing POA neurons, PGDS-Cre mouse brains with Cre-dependent hM3Dq, hM4Di, or mCherry expressing in POA (method described in

"Stereotactic injection" section) were sectioned for recording. Neurons with vector expression were labeled with mCherry. Identical recording protocol was used as above, except that the bath temperature was maintained at 36°C throughout the recording. After recording of the baseline firing for 1–2 mins, the neurons were challenged with clozapine (1 μM, 1 min, Tocris, Bristol, UK) followed by immediate wash-out with normal ACSF. The recording usually lasted for 6 min. 10 neurons each were recorded from PGDS-Cre/hM3Dq, hM4Di, or mCherry slices.

To evaluate the response of vMPO neurons to PGD_2, we used B6 WT mice to generate vMPO brain slices. Identical recording protocol and analysis method were used as above, except that 1) the treatment of PGD_2 (20 μM, < 10 s, Cayman Chemical, Ann Arbor, MI) was delivered to the bottom of 3rd ventricle, where the DP1 receptors were clustered; 2) recording was performed in bath of ACSF containing DNQX (20 μM), AP5 (50 μM), SR 95531 (20 μM), and MK-0524 (100 nM, Cayman Chemical, Ann Arbor, MI) or its vehicle (0.1% DMSO). 7 neurons were recorded each in bath containing MK-0524 or vehicle.

To demonstrate the projection from PGDS-expressing POA neurons to vMPO, we injected AAV vectors expressing Cre-dependent ChR2 or mCherry into medial and lateral POA of PGDS-Cre mice (method described in "Stereotactic injection" section). Three weeks later, vMPO slices were sectioned for recording. Identical recording protocols and analysis methods were used as above, except that 1) blue excitation laser (30 s) was applied to illuminate the entire optical field under 60x water objective; 2) recording was performed in bath of ACSF containing DNQX (20 μM), AP5 (50 μM), SR 95531 (20 μM), and MK-0524 (100 nM, Cayman Chemical, Ann Arbor, MI) or vehicle control (0.1% DMSO). Forty-two neurons were recorded from mice with ChR2 vector injection (24 with MK-0524 in bath and 18 with vehicle in bath); 18 neurons were recorded from control mice with mCherry vector injection.

Single-cell RNA-seq—After recording, the cellular component of each neuron was captured into the electrode pipet by delivering a gentle negative pressure, and then transferred into a PCR tube containing reaction buffer for reverse transcription (RT) by breaking the glass tip and delivering a gentle positive pressure. The cDNA library was prepared immediately; or the samples were frozen in liquid N_2 for later processing (see also Figures S2H–S2O for details). An established protocol of SMART-Seq2 was adapted (Picelli et al., 2013, 2014), with minor modification to incorporate the internal solution for whole-cell patch-clamp (key reagents include SUPERaseIn and RNaseOUT from Thermo Fisher, South San Francisco, CA; ProtoScript II, DTT, and $MgCl_2$ from NEB, Ipswich, MA; betaine from MilliporeSigma, Burlington, MA; KAPA HiFi HotStart ReadyMix from Roche, Basel, Switzerland; template switch oligo from Exiqon/Qiagen, Hilden, Germany; oligo dT and PCR primers from IDT, San Jose, CA). The cDNA libraries were purified with AMPure XP beads (Beckman Coulter, Indianapolis, IN), and their mass concentrations were measured with Qubit (Thermo Fisher, South San Francisco, CA). Bioanalyzer high sensitive DNA chip (Agilent, Santa Clara, CA) was also applied to check the distribution of fragments in each individual library. Libraries of low concentration of cDNA or with distorted curve on Bioanalyzer were discarded. 96 cDNA libraries were processed in preparation for sequencing. Tagmentation was performed following the standard protocol of Illumina

Nextera XT kit (Illumina, San Diego, CA). Sequencing libraries were purified with AMPure XP beads and their final concentrations were measured with Qubit; the 96 libraries were pooled with equal molar amount; and the pooled library was size-selected by BluePippin (Sage, Beverly, MA) for fragments of 300–500 bp. The sequencing of cDNAs was performed with Illumina HiSeq 4000, SE50.

Immunostaining—Mice subjected for immunostaining were perfused with 4% paraformaldehyde (PFA) in phosphate-buffered saline (PBS, 137.0 mM NaCl, 2.7 mM KCl, 10.0 mM Na_2HPO_4, 1.8 mM KH_2PO_4, pH 7.4) through the left ventricle. After post-fix in 4% PFA for overnight, the brain was sectioned into 40 μm slices in PBS with a vibrating blade microtome (Leica, Wetzlar, DE). After washing in Tris-buffered saline (TBS, 50 mM Tris, 150 mM NaCl, pH 7.4) for 3 times, heat induced epitope retrieval was performed by incubating the slices in 10 mM Na-citrate with 0.05% Tween 20, pH 6.0, at 80°C, for 30 min. Upon cooling down, the brain slices were washed 3 times in TBS with 0.3% Triton 100 (TBS-T). The brain slices were first blocked in the blocking buffer (TBS with 0.3% Triton 100, 10% normal donkey serum, and 2% bovine serum albumin) at room temperature for 2 hours, and then incubated with primary antibodies against L-PGDS (mouse anti PGD_2 synthase (F-7), 1:200, Santa Cruz, Dallas, TX, Cat #sc-390717, RRID:AB_2800545), CaMKI (guinea pig anti CaMKI, 1:500, Synaptic Systems, Goettingen, Germany, Cat #211 005, RRID:AB_2070109), tdTomato (rat anti tdTomato, 1:500, Kerafast, Boston, MA, Cat # EST203, RRID:AB_2732803), mCherry (rabbit anti mCherry, 1:1000 or 1:5000, Abcam, Cambridge, UK, Cat #ab167453, RRID:AB_2571870), DP1 (rabbit anti DP1, 1:200, Cayman Chemical, Ann Arbor, MI, Cat #101640, RRID:AB_10078133), BDNF (sheep anti BDNF, 1:100, MilliporeSigma, Burlington, MA, Cat #AB1513P, RID:AB_2064329), PACAP (mouse anti PACAP, 1:500, Santa Cruz, Dallas, TX, Cat #sc-166180, RRID:AB_2289234), and/or GFP (chicken anti GFP, 1:2000, Aves Labs, Davis, CA, Cat # GFP-1020, RRID:AB_10000240) at 4°C overnight. After washing in TBS-T for 3 times, brain slices were incubated with secondary antibodies of donkey anti mouse IgG conjugated with Alexa 488 (1:1000, Thermo Fisher, South San Francisco, CA), donkey anti rat IgG conjugated with RRX (1:1000, Jackson ImmunoResearch, West Grove, PA), donkey anti guinea pig IgG conjugated with ALEXA 647 (1:1000, Thermo Fisher, South San Francisco, CA), donkey anti sheep IgG conjugated with Alexa 488 (1:1000, Thermo Fisher, South San Francisco, CA), donkey anti rabbit IgG conjugated with RRX (1:1000, Jackson ImmunoResearch, West Grove, PA), donkey anti mouse IgG conjugated with Alexa 647 (1:1000, Thermo Fisher, South San Francisco, CA), and/or donkey anti chicken IgY conjugated with Alexa 488 (1:1000, Thermo Fisher, South San Francisco, CA), plus DAPI (1:5000, MilliporeSigma, Burlington, MA). After washing in TBS for 3 times, the brain slices were mounted onto glass slides and coated with Fluoroshield (MilliporeSigma, Burlington, MA). The specimen was imaged with confocal microscope (Leica SP5, Wetzlar, DE) after drying.

Chemogenetics—After recovery from virus injection, a temperature probe (G2 E-Mitter, Starr Life Sciences, Oakmont, PA) was implanted into the mouse' abdominal cavity. After recovery for another week, the mouse was single-housed in a thermal-controlled incubator (Power Scientific, Warminster, PA) with normal lighting schedule and ambient temperature

of 22°C for at least overnight to habituate to the environment; food and water were served ad libitum. The cage sat on an ER4000 Energizer/Receiver (Starr Life Sciences, Oakmont, PA), which powers the E-Mitter and receives the measurement data. The body temperature (T_c) and locomotor activity of the mouse were recorded with VitalView (Starr Life Sciences, Oakmont, PA) with one sampling per min. On the experimental day, at CT 0.5 or CT 11.5, the mouse was anesthetized with isoflurane, and Intraperitoneal (IP) injected with vehicle (sterile saline), or clozapine (10 μg/kg body weight)(Gomez et al., 2017). 2 days later at the same time, another injection of reagent different from that used for the 1st injection was delivered with the same procedure. In total, the mouse body temperature was recorded for at least 8 days. When finished, the mouse brains were sectioned for validation of vector expression, and/or electrophysiological recordings.

LC-MS/MS—The brain slices of PGDS-Cre mice were prepared as described above. After a recovery period of 90 min at room temperature, brains slices of POA or thalamus were transferred into a heating chamber (Warner Instrument, Hamden, CT) with constant perfusion of ACSF. The treatments of TTX (1 μM, Tocris, Bristol, UK), Ca^{2+}-free ACSF (0 mM Ca^{2+} ACSF with 10 mM EGTA), synaptic transmission blockers of DNQX (20 μM), AP5 (50 μM), and SR 95531 (20 μM), AT-56 (20 μM, Cayman Chemical, Ann Arbor, MI) (Irikura et al., 2009) or its vehicle (5% DMSO and 5% 2-Hydroxypropyl-β-cyclodextrin in sterile saline) were delivered during this period, if applicable. After 20 min washing (and treatment) at 30°C, the perfusion was stopped, and the bath temperature in the chamber was maintained at 33°C, 36°C, or 39°C for 5 or 30 min. The incubation of the brain slices was performed at CT 6–8. The brain slices were harvested, flash-frozen in liquid N_2, and stored in −80°C for further processing.

The investigator performing the following procedure was blind to the treatment of the brain slice samples. Lipid extraction was performed according to Farias and colleagues (Farias et al., 2008) with slight modification. 100 pg of deuterated internal standards, *d4*-PGD_2 and *d4*-PGE_2 (Cayman Chemical, Ann Arbor, MI), were added to each tissue sample. After homogenization and extraction, dried lipid samples were dissolved in 100 μl of 0.7 mM ammonium formate in 68% aqueous methanol. 40 μl of each sample was injected into a C18 HPLC column (Kinetex 5 μm 100 Å, 150 × 4.6 mm, Phenomenex) and eluted at a flow rate of 1 ml/min with 0.8 mM ammonium acetate in 28% aqueous acetonitrile. A quadrupole linear-ion trap mass spectrometer (AB Sciex QTRAP 6500) was connected to a Shimadzu HPLC system as a detector. PGD_2 and PGE_2 were separated as two non-overlapping peaks between retention time 3 to 5 min. Mass spectrometric analyses were performed in negative-ion mode using multiple reaction monitoring (MRM) of the following specific *m*/*z* (precursor → product) transitions: 351 → 189 (PGD_2); 351 → 271 (PGE_2); 355 → 193 (*d4*-PGD_2); 355 → 275 (*d4*-PGE_2). Remaining insoluble material from the lipid extraction was dried down and subjected to trypsin digestion (40 μg trypsin per sample in 20 mM Tris-HCl, pH 7.5, 37°C for 2 days). After centrifuging (16,000×g for 15 min at 4°C) to remove particulates, released peptides were quantified via the BCA protein assay (Thermo Fisher, South San Francisco, CA) and the absolute amount of protein was used to normalize lipid levels.

Western Blot—The brain slices of POA, thalamus, cortex, striatum, and hippocampus were prepared as described above, frozen immediately on dry ice and stored at −80 °C. Frozen tissue samples were mixed with 100 μL of lysis buffer (10 mM Tris-HCl, 150 mM NaCl, 1% Triton X-100, 0.5% sodium deoxycholate, 0.1% SDS, 4 mM EDTA, 0.5 mM TCEP, and 1x Complete protease inhibitor cocktail (Roche, Basel, Switzerland), pH 7.5), incubated on ice for 15 min and homogenized with a plastic pestle. After another 15 min of incubation on ice, the samples were centrifuged at 16,000 ×g for 15 min at 4 °C and the supernatants were transferred to fresh tubes. Protein content of each sample was determined by Bradford assay, after which equal amounts of protein was mixed with NuPAGE LDS sample buffer (Thermo-Fisher, South San Francisco, CA) supplemented with 0.1 M DTT. 12 μg of total protein from each sample was resolved in NuPAGE 4–12% Bis-Tris protein gels with MES running buffer (Thermo Fisher, South San Francisco, CA) and transferred to Immobilon-P membranes (MilliporeSigma, Burlington, MA) using a Trans-Blot Turbo transfer system (Bio-Rad, Hercules, CA). Membranes were blocked with 5% non-fat milk prepared in TBST (10 mM Tris-HCl, 150 mM NaCl, and 0.1% Tween-20, pH 7.5) and probed with mouse anti-PGD2 synthase (F-7, 1:1000 dilution, Santa Cruz, Dallas, TX) at 4 °C for overnight. Membranes were further incubated with anti-mouse IgG-HRP secondary antibody (1:28000 dilution, Jackson ImmunoResearch, West Grove, PA) and developed with SuperSignal West Femto Chemiluminescent Substrate (Thermo Fisher, South San Francisco, CA). For loading control, membranes were treated with 30% hydrogen peroxide for 15 min at 37 °C to inactivate HRP activity, washed with ddH_2O, reprobed with HRP-Conjugated GAPDH Antibody (1:20000 dilution, Proteintech, Rosemont, IL) and developed with Pierce ECL Western Blotting Substrate (Thermo Fisher, South San Francisco, CA). A C-DiGit blot scanner (LI-COR) was used to visualize the chemiluminescent signal and Image Studio Software (LI-COR) was used for quantification.

ICV injection and body temperature measurement—B6 WT mouse was implanted with a temperature probe G2 E-Mitter into the abdominal cavity and a brain guide cannula (PlasticsOne, Roanoke, VA) into the lateral ventricle (AP −0.4, ML −0.8, DV 2.4) on the same day. After recovery for at least 6 days, the mouse was single-housed in a thermal-controlled incubator with normal lighting schedule and ambient temperature of 22°C for at least overnight to habituate to the environment; food and water were served ad libitum. The cage sat on an ER4000 Energizer/Receiver, which powers the E-Mitter and receives the measurement data. On the experimental day, at CT 4–5, the mouse was anesthetized with isoflurane to install injection cannula, and IP injected with vehicle (5% DMSO and 5% 2-Hydroxypropyl-β-cyclodextrin in sterile saline), MK-0524 (4 mg/kg body weight) (Cheng et al., 2006), or AT-56 (20 mg/kg body weight) (Irikura et al., 2009). The T_c and locomotor activity of the mouse were recorded with VitalView with one sampling per min. After a baseline recording for at least 60 min, the mouse was intracerebroventricular (ICV) injected with vehicle (10% DMSO in sterile saline), PGD_2 (2 nmol in 1μl), or PGE_2 (2 nmol in 1μl, Cayman Chemical, Ann Arbor, MI). The assignment of the treatment to the animals is random, but the replicates of each treatment are the same ($N = 6$). The T_c of the mouse was recorded for at least 3 hours until the injection cannula was removed. When finished, the mouse brains were sectioned to validate the correct position of cannula implantation.

CRISPRi mediated *Ptgds* knockdown in POA of mouse—To clone the sgRNAs targeting *Ptgds* for CRISPRi, three candidates were selected from a published sgRNA libraries to minimize potential off-target effects(Horlbeck et al., 2016). The sgRNAs were designed to target within −25 and 500 bp of the TSS and contains 19 bp followed by an NGG PAM. The sgRNAs sequences were ordered from IDT (Coralville, IA) with compatible restriction enzyme overhangs for cloning into a pSico based lentiviral sgRNA expression vector in which the sgRNA is driven by a mouse U6 promoter. The vector also expresses GFP and Hygromycin resistance from a short EF1a promoter. The sgRNA expression vector was prepared by restriction digest with AarI (Thermo Fisher, South San Francisco, CA) at 37°C overnight, followed by 1% agarose gel excision of the digested backbone via NucleoSpin columns (Macherey-Nagel, Bethlehem, PA). The annealed sgRNAs and the digested backbone were ligated with T4 (NEB, Ipswich, MA) overnight at 16°C, followed by transformation into homemade chemically competent Stellar cells. The minipreped sgRNA vectors were sequenced by Quintara Bioscience (South San Francisco, CA) to confirm correctly cloned sequence.

Lentivirus was produced by UCSF Viracore, with the procedure as: HEK293T cells were seeded at 65,000 cells per cm^2 in 10 cm dishes in 10 mL media (DMEM, 10% fetal bovine serum, 1% Sodium Pyruvate, 1% Nonessential Amino Acids) and incubated overnight at 37°C, 5% CO_2. The next morning, 6 μg sgRNA plasmid, 3 μg psPAX2 (Addgene #12260), 3 μg pMD2.G (Addgene #12259) and 25 μL jetPRIME (Polyplus Transfection, Illkirch, FR) were mixed into 850μL sterile water with 1x jetPRIME buffer, vortexed and incubated for 10 min at RT and added to the cells. At 72 h post-transfection, supernatant was harvested, passed through 0.45 um filters and ultracentrifuged at 25,000 rpm for 2 h to collect the virus. The viral pellet was diluted in sterile PBS, aliquoted, and stored at −80°C. The virus was tittered on HEK293T cells with FACS (Attune™ NxT Flow Cytometer) and the titers were ~$4*10^8$ TU/ml.

All sgRNAs targeting *Ptgds* were validated by transduction of mouse E14 ESCs, stably expressing dCas9-KRAB. RNA was harvested 10 days after transduction and all sgRNAs candidates displayed robust knock down of *Ptgds* (data not shown). In the following *in vivo* knockdown experiments, the sgRNAs targeting *Ptgds* with the sequence TGCTCCATGAGCCCCTCAT and the non-targeting control with the sequence GCCTGGACCTAACGTCCGAG were used to prepare lentivirus for mouse brain injection.

The dCas9-KRAB mice were injected with lentivirus vector of 1.0 μl into medial and lateral POA (bilateral, stereotactic coordinates AP 0.1, ML ±0.3, DV 5.5). After one week's recovery, they were implanted with a temperature probe G2 E-Mitter into the abdominal cavity. After another recovery for 1 week, the mouse was single-housed in a thermal-controlled incubator with normal lighting schedule and ambient temperature of 22°C; food and water were served ad libitum. The cage sat on an ER4000 Energizer/Receiver, which powers the E-Mitter and receives the measurement data. The T_c and locomotor activity of the mouse were recorded with VitalView with one sampling per min, for at least 10 days. The periodogram of the T_c oscillation was analyzed with ClockLab. The T_c of the mice in test were closely monitored; if it dropped below 25°C, the mouse was euthanized

immediately (as a humane endpoint). When finished, the mouse brains were sectioned to validate the correct position of injection, and to evaluate the gene knockdown efficiency.

When testing the mice in elevated ambient temperature, the animals were exposed to ambient temperature of 37°C for 4 hours on day 14.

QUANTIFICATION AND STATISTICAL ANALYSIS

Electrophysiology—To measure the temperature sensitivity of a neuron, the spontaneous action potentials (SAP) were counted at the steady state of 33°C, 36°C, and 39°C, within one sweep of 15 sec; the slope of firing frequency change in response to temperature change was calculated by linear regression of the firing frequency plotted against the test temperatures. If the neuron was silent at a certain temperature (SAP = 0 Hz, most likely ~33°C), or exhibited obviously seizure like firing (SAP > 20 Hz, low amplitude, most likely ~39°C), the data at the certain temperature point were removed from linear regression. The criterion(Boulant and Dean, 1986) for “warm-sensitive” neurons is SAP frequency increasing with temperature elevation at a rate > +0.8 Hz/°C, while the criterion (Boulant and Dean, 1986) for “cold-sensitive” neurons is SAP frequency change < −0.6 Hz/°C; neurons with mild changes of firing frequency are defined as “temperature-insensitive”; neurons with no spontaneous action potentials are defined as “silent”. For silent neurons, the resting membrane potential (V_m) was measured at 3 different test temperature, and the V_m change over temperature (dV_m / dT) were calculated by linear regression; the spontaneous post-synaptic potentials (if applicable) were counted during the period of incubation temperature increase, with temperature bin of 1°C; the event counts at each temperature window were fit to Gauss distribution, and the adjusted R-squared (R^2) was calculated. Silent neurons with $|dV_m / dT| > 1$ mV/°C or $R^2 > 0.9$ are classified as “temperature-sensitive silent neurons”, while the rest of silent neurons with mild change in V_m and spontaneous post-synaptic potentials over temperature rising are classified as “temperature-insensitive silent neurons”.

For recordings with treatments of clozapine or PGD_2, the SAP frequencies were calculated from 1 sweep (15 s) before the treatment and 1 sweep afterwards. For recordings with optogenetics stimulation, the SAP frequencies were calculated from 1 sweep (15 s) before, 1 sweep during, and 1 sweep after the laser illumination.

Bioinformatics—Quality control for sequencing was assessed using FastQC; raw reads were trimmed with R-package scythe for adapter contamination, and with sickle for low quality reads. Reads were aligned to the mouse reference genome sequence mm10 with STAR, using UCSC annotation from iGenomes. Raw read counts were generated by STAR. Gene expression values were normalized based on library size as counts per million reads (CPM).

Differential expression (DE) analysis was conducted using the Bioconductor package edgeR. The model of Negative Binomial Distribution was employed; normalization was conducted using the TMM method; estimation and testing were conducted using the quasilikelihood method. The DE analysis includes 78 libraries with known temperature-sensitivity based

upon electrophysiology; they were classified into 5 categories, as described in main text, Figure S3A, and Table S1.

A MATLAB toolbox SCell was used to analyze the single-cell transcriptomes (Diaz et al., 2016). Simpsons Diversity Index was applied to evaluate the complexity of each library, through which 84 libraries passed the criteria and 12 libraries were filtered out. Furthermore, the index of dispersion (IOD) of each individual gene (log-transformed CPM values) in the 84 libraries was calculated; genes of the bottom 25%, which exhibit less variance in different libraries (low IOD value), were excluded from the following PCA analysis. In addition, genes expressed in fewer than 10% of the libraries were also excluded. The remaining 12912 genes from 84 libraries were subjected to PCA. These 84 cDNA libraries correspond to the transcriptomes of 68 neurons that experienced patch-clamp recording for ~10 min ("fresh" in Figure S2) and 16 neurons that were harvested immediately after membrane break-through via the patch clamp electrode without recording ("pick" in Figure S2). The PCA of the 84 libraries (Figure S2O) demonstrates that the patch-clamp recording and temperature variations over the course of 10 min did not alter the gene expression pattern of the neurons in POA. Further PCA of the 68 libraries with designated temperature-sensitivity of the neurons and the cluster analysis (K-means) was also performed with SCell, as described in the main text.

Immunostaining—In experiments staining L-PGDS and CaMKI in POA of WT mice (Figure 1O), a total of 264 cells, based upon nucleus staining with DAPI, were collected from 3 independent replicates. The percentage of cells with 1) L-PGDS staining only, 2) CaMKI staining only, 3) both L-PGDS and CaMKI stainings, or 4) neither of the two staining, over the total cell numbers was calculated to quantify the expression of the two target proteins.

In experiments staining tdTomato, L-PGDS, and CaMKI in POA of PGDS-Cre/Ai14 mice (Figures 2A, 2B, and S3C), a total of 459 cells, based upon nucleus staining with DAPI, were collected from 3 independent replicates. The cells were first classified into 2 categories, with or without tdTomato staining. Then the percentage of cells with 1) L-PGDS staining only, 2) CaMKI staining only, 3) both L-PGDS and CaMKI staining, or 4) neither of the two staining, in each of 2 categories was calculated separately, to quantify the overlap expression of tdTomato with L-PGDS or CaMKI.

In experiments staining mCherry, L-PGDS, and CaMKI in POA of PGDS-Cre/AAV-mCherry mice (Figure S4B and S4C), identical quantification method was used as above with a total of 416 cells collected from 3 independent replicates.

In experiments staining DP1, BDNF, and PACAP in vMPO and POA of WT mice (Figures 6B and S6C–S6F), a total of 432 vMPO cells and 542 of POA cells, were collected from 3 independent replicates (each pair of vMPO and POA slices was harvested from the same mouse, 3 mice in total). The percentage of cells with BDNF staining over total cell numbers (based upon nucleus staining with DAPI) was calculated in vMPO and POA; the percentage of cells with both DP1 and BDNF staining over the number of cells with BDNF staining was calculated in vMPO and POA. Cells with DP1 only but not BDNF staining were not

detected in the 3 replicates. The staining of DP1 and PACAP in putative dendrite along the 3rd ventricle is not quantified, because of the difficulty in delineating the neuronal processes away from their cell bodies.

In experiments staining GFP and L-PGDS in POA of dCas9-KRAB mice with sgRNA injection (Figures 7B–7D), a total of 451 cells were collected from *Ptgds*-sgRNA group and a total of 456 cells were collected control-sgRNA group (3 independent replicates in each group). The percentage of GFP-positive cells was used to quantify the transfection rate (marked with GFP), while the percentage L-PGDS-positive cells was used to quantify the gene knockdown efficiency.

LC-MS/MS—Peak areas from each analyte and their corresponding deuterated spiked-in standards were obtained from Analyst software (AB Sciex) to calculate the amount of lipid hormones in each sample, which was further normalized to the total protein level in each sample.

Body temperature measurement—In chemogenetics (Figures 3), the T_c was compared between clozapine treatment and its vehicle 2 hours before till 6 hours after IP injection. In ICV injection (Figure 5), the baseline T_c was determined from the average of recording for 30 min before the ICV injection, and the change in body temperature (ΔT_c) following the ICV over the course of 2 hours was calculated and compared in different groups. In CRISPRi-mediated knockdown experiment with elevated ambient temperature increase (Figures 7L and 7M), the baseline T_c was determined from the average of recording for 60 min before the temperature manipulation, and ΔT_c following the ambient temperature increase over the course of 4 hours was calculated and compared between sgRNA of NT *vs. Ptgds*.

Statistics—Sample sizes were chosen on the basis of similar experiments in the field, and Power Analysis (online calculator) with preliminary results; 7–10 replicates for electrophysiology; 3 replicates for immunostaining; 6 replicates for biochemistry assay, and 6–8 replicates for measurement in live animals. Statistical significance was assayed by Student's t-test, Chi square, log rank, or One-way ANOVA with GraphPad Prism. *, $P < 0.05$; **, $P < 0.01$. Variance was examined by an F-test. Data are represented as mean ± s.e.m.

Supplementary Material

Refer to Web version on PubMed Central for supplementary material.

ACKNOWLEDGEMENTS

We thank Drs. Charles Kim and Mu He for technology introduction at the inception of this work, anonymous colleagues at SEQanswers.com (user ID: simone78, jwfoley, and bplevi) for advice about cDNA library generation, Dr. Eric Chow and Center for Advanced Technology at UCSF for sequencing facility, UC Davis Bioinformatics Core for bioinformatics facility, Dr. Robert Murphy and the Mass Spectrometry Lipidomics Core Facility at University of Colorado Denver for advice about lipid hormone measurement, Drs. Jason Cyster, Yong Huang, and Qiyun Yang for the LC-MS/MS facility, Dr. Sami Tuomivaara for biochemistry and statistics consultation, Ms. Stacey Phan and UCSF Viracore for lentivirus preparation, Ms. Alondra Hurtado for mouse breeding, and Drs. Ying-hui Fu, Louis J. Ptacek, and Guangsen Shi for the support of analytical software ClockLab. The mouse line

FVB.Cg-Ptgds<tm1(cre)Gvn>/GvnRbrc was generated by Dr. Marco Giovannini, and provided by the RIKEN BRC through the National Bio-Resource Project of the MEXT, Japan. The pAAV-hSyn-DIO-hM3D(Gq)-mCherry, pAAV-hSyn-DIO-hM4D(Gi)-mCherry, and pAAV-hSyn-DIO-mCherry, were gifts from Dr. Bryan Roth (Addgene viral prep # 44361-AAV8, # 44362-AAV8, and # 50459-AAV8)(Krashes et al., 2011). The pAAV-EF1a-double floxed-hChR2(H134R)-mCherry-WPRE-HGHpA was a gift from Dr. Karl Deisseroth (Addgene viral prep # 20297-AAV8). psPAX2 (Addgene #12260) and pMD2.G (Addgene #12259) were gifts from Dr. Didier Trono, Parts of the graphs in the figures and graphical abstract were adapted from the Allen Mouse Brain Reference Atlas and Warner Instruments product demo. Y.N.J. and L.Y.J. are Howard Hughes Medical Institute Investigators. The research was supported by R01NS069229 to L.Y.J.

REFERENCE

Abbott SB, Machado NL, Geerling JC, and Saper CB (2016). Reciprocal control of drinking behavior by median preoptic neurons in mice. J Neurosci 36, 8228–8237. [PubMed: 27488641]

Boulant JA, and Dean JB (1986). Temperature receptors in the central nervous system. Annu Rev Physiol 48, 639–654. [PubMed: 3010828]

Cadwell CR, Palasantza A, Jiang X, Berens P, Deng Q, Yilmaz M, Reimer J, Shen S, Bethge M, Tolias KF, et al. (2016). Electrophysiological, transcriptomic and morphologic profiling of single neurons using Patch-seq. Nat Biotechnol 34, 199–203. [PubMed: 26689543]

Carlisle HJ (1966). Behavioural Significance of Hypothalamic Temperature-Sensitive Cells. Nature 209, 1324–1325. [PubMed: 5956045]

Carlisle HJ, and Laudenslager ML (1979). Observations on the thermoregulatory effects of preoptic warming in rats. Physiol Behav 23, 723–732. [PubMed: 504468]

Cheng K, Wu TJ, Wu KK, Sturino C, Metters K, Gottesdiener K, Wright SD, Wang Z, O'Neill G, Lai E, et al. (2006). Antagonism of the prostaglandin D2 receptor 1 suppresses nicotinic acid-induced vasodilation in mice and humans. Proc Natl Acad Sci U S A 103, 6682–6687. [PubMed: 16617107]

Chung S, Weber F, Zhong P, Tan CL, Nguyen TN, Beier KT, Hörmann N, Chang WC, Zhang Z, Do JP, et al. (2017). Identification of preoptic sleep neurons using retrograde labelling and gene profiling. Nature 545, 477–481. [PubMed: 28514446]

Conti B, Sanchez-Alavez M, Winsky-Sommerer R, Morale MC, Lucero J, Brownell S, Fabre V, Huitron-Resendiz S, Henriksen S, Zorrilla EP, et al. (2006). Transgenic mice with a reduced core body temperature have an increased life span. Science 314, 825–828. [PubMed: 17082459]

Deurveilher S, and Semba K (2005). Indirect projections from the suprachiasmatic nucleus to major arousal-promoting cell groups in rat: implications for the circadian control of behavioural state. Neuroscience 130, 165–183. [PubMed: 15561433]

Diaz A, Liu SJ, Sandoval C, Pollen A, Nowakowski TJ, Lim DA, and Kriegstein A (2016). SCell: integrated analysis of single-cell RNA-seq data. Bioinformatics 32, 2219–2220. [PubMed: 27153637]

Eberwine J, and Bartfai T (2011). Single cell transcriptomics of hypothalamic warm sensitive neurons that control core body temperature and fever response Signaling asymmetry and an extension of chemical neuroanatomy. Pharmacol Ther 129, 241–259. [PubMed: 20970451]

Farias SE, Basselin M, Chang L, Heidenreich KA, Rapoport SI, and Murphy RC (2008). Formation of eicosanoids, E2/D2 isoprostanes, and docosanoids following decapitation-induced ischemia, measured in high-energy-microwaved rat brain. J Lipid Res 49, 1990–2000. [PubMed: 18503030]

Fuzik J, Zeisel A, Máté Z, Calvigioni D, Yanagawa Y, Szabó G, Linnarsson S, and Harkany T (2016). Integration of electrophysiological recordings with single-cell RNA-seq data identifies neuronal subtypes. Nat Biotechnol 34, 175–183. [PubMed: 26689544]

Gomez JL, Bonaventura J, Lesniak W, Mathews WB, Sysa-Shah P, Rodriguez LA, Ellis RJ, Richie CT, Harvey BK, Dannals RF, et al. (2017). Chemogenetics revealed: DREADD occupancy and activation via converted clozapine. Science 357, 503–507. [PubMed: 28774929]

Gordon C (2012). Thermal physiology of laboratory mice: Defining thermoneutrality. J Therm Biol 37, 654–685.

Griffin JD, and Boulant JA (1995). Temperature effects on membrane potential and input resistance in rat hypothalamic neurones. J Physiol (Lond) 488 (Pt 2), 407–418. [PubMed: 8568679]

Heimberg G, Bhatnagar R, El-Samad H, and Thomson M (2016). Low Dimensionality in Gene Expression Data Enables the Accurate Extraction of Transcriptional Programs from Shallow Sequencing. Cell Systems 2, 239–250. [PubMed: 27135536]

Hemingway A, Forgrave P, and Birzis L (1954). Shivering suppression by hypothalamic stimulation. J Neurophysiol 17, 375–386. [PubMed: 13175054]

Horlbeck MA, Gilbert LA, Villalta JE, Adamson B, Pak RA, Chen Y, Fields AP, Park CY, Corn JE, Kampmann M, et al. (2016). Compact and highly active next-generation libraries for CRISPR-mediated gene repression and activation. Elife 5.

Irikura D, Aritake K, Nagata N, Maruyama T, Shimamoto S, and Urade Y (2009). Biochemical, functional, and pharmacological characterization of AT-56, an orally active and selective inhibitor of lipocalin-type prostaglandin D synthase. J Biol Chem 284, 7623–7630. [PubMed: 19131342]

Ivanov AI, and Romanovsky AA (2004). Prostaglandin E2 as a mediator of fever: synthesis and catabolism. Front Biosci 9, 1977–1993. [PubMed: 14977603]

Kalamarides M, Stemmer-Rachamimov AO, Niwa-Kawakita M, Chareyre F, Taranchon E, Han ZY, Martinelli C, Lusis EA, Hegedus B, Gutmann DH, et al. (2011). Identification of a progenitor cell of origin capable of generating diverse meningioma histological subtypes. Oncogene 30, 2333–2344. [PubMed: 21242963]

Kelso SR, and Boulant JA (1982). Effect of synaptic blockade on thermosensitive neurons in hypothalamic tissue slices. Am J Physiol 243, R480–90. [PubMed: 7137377]

Krashes MJ, Koda S, Ye C, Rogan SC, Adams AC, Cusher DS, Maratos-Flier E, Roth BL, and Lowell BB (2011). Rapid, reversible activation of AgRP neurons drives feeding behavior in mice. J Clin Invest 121, 1424–1428. [PubMed: 21364278]

Lazarus M, Yoshida K, Coppari R, Bass CE, Mochizuki T, Lowell BB, and Saper CB (2007). EP3 prostaglandin receptors in the median preoptic nucleus are critical for fever responses. Nat Neurosci 10, 1131–1133. [PubMed: 17676060]

Magoun HW, Harrison F, Brobeck JR, and Ranson SW (1938). Activation of heat loss mechanisms by local heating of the brain. Journal of Neurophysiology 1, 101–114.

Matsumura H, Nakajima T, Osaka T, Satoh S, Kawase K, Kubo E, Kantha SS, Kasahara K, and Hayaishi O (1994). Prostaglandin D2-sensitive, sleep-promoting zone defined in the ventral surface of the rostral basal forebrain. Proc Natl Acad Sci U S A 91, 11998–12002. [PubMed: 7991572]

Moffitt JR, Bambah-Mukku D, Eichhorn SW, Vaughn E, Shekhar K, Perez JD, Rubinstein ND, Hao J, Regev A, Dulac C, et al. (2018). Molecular, spatial, and functional single-cell profiling of the hypothalamic preoptic region. Science 362.

Morrison SF (2016). Central control of body temperature. [version 1; referees: 3 approved]. F1000Res 5.

Nakamura K (2011). Central circuitries for body temperature regulation and fever. Am J Physiol Regul Integr Comp Physiol 301, R1207–28. [PubMed: 21900642]

Ohinata K, Suetsugu K, Fujiwara Y, and Yoshikawa M (2006). Activation of prostaglandin E receptor EP4 subtype suppresses food intake in mice. Prostaglandins Other Lipid Mediat 81, 31–36. [PubMed: 16997129]

Ohinata K, Takagi K, Biyajima K, Fujiwara Y, Fukumoto S, Eguchi N, Urade Y, Asakawa A, Fujimiya M, Inui A, et al. (2008). Central prostaglandin D(2) stimulates food intake via the neuropeptide Y system in mice. FEBS Lett 582, 679–684. [PubMed: 18258196]

Onoe H, Watanabe Y, Ono K, Koyama Y, and Hayaishi O (1992). Prostaglandin E2 exerts an awaking effect in the posterior hypothalamus at a site distinct from that mediating its febrile action in the anterior hypothalamus. J Neurosci 12, 2715–2725. [PubMed: 1613554]

Picelli S, Björklund ÅK, Faridani OR, Sagasser S, Winberg G, and Sandberg R (2013). Smart-seq2 for sensitive full-length transcriptome profiling in single cells. Nat Methods 10, 1096–1098. [PubMed: 24056875]

Picelli S, Faridani OR, Björklund AK, Winberg G, Sagasser S, and Sandberg R (2014). Full-length RNA-seq from single cells using Smart-seq2. Nat Protoc 9, 171–181. [PubMed: 24385147]

Pollen AA, Nowakowski TJ, Shuga J, Wang X, Leyrat AA, Lui JH, Li N, Szpankowski L, Fowler B, Chen P, et al. (2014). Low-coverage single-cell mRNA sequencing reveals cellular heterogeneity

and activated signaling pathways in developing cerebral cortex. Nat Biotechnol 32, 1053–1058. [PubMed: 25086649]

Poulin JF, Tasic B, Hjerling-Leffler J, Trimarchi JM, and Awatramani R (2016). Disentangling neural cell diversity using single-cell transcriptomics. Nat Neurosci 19, 1131–1141. [PubMed: 27571192]

Refinetti R, and Menaker M (1992). The circadian rhythm of body temperature. Physiol Behav 51, 613–637. [PubMed: 1523238]

Romanovsky AA, and Garami A (2010). Prostaglandin riddles in energy metabolism: E is for excess, D is for depletion. Focus on "Food deprivation alters thermoregulatory responses to lipopolysaccharide by enhancing cryogenic inflammatory signaling via prostaglandin D2". Am J Physiol Regul Integr Comp Physiol 298, R1509–11. [PubMed: 20410482]

Rossitto M, Ujjan S, Poulat F, and Boizet-Bonhoure B (2015). Multiple roles of the prostaglandin D2 signaling pathway in reproduction. Reproduction 149, R49–58. [PubMed: 25269616]

Saper CB, Romanovsky AA, and Scammell TE (2012). Neural circuitry engaged by prostaglandins during the sickness syndrome. Nat Neurosci 15, 1088–1095. [PubMed: 22837039]

Smith WL, Urade Y, and Jakobsson PJ (2011). Enzymes of the cyclooxygenase pathways of prostanoid biosynthesis. Chem Rev 111, 5821–5865. [PubMed: 21942677]

Song K, Wang H, Kamm GB, Pohle J, Reis FC, Heppenstall P, Wende H, and Siemens J (2016). The TRPM2 channel is a hypothalamic heat sensor that limits fever and can drive hypothermia. Science 353, 1393–1398. [PubMed: 27562954]

Tan CL, Cooke EK, Leib DE, Lin YC, Daly GE, Zimmerman CA, and Knight ZA (2016). Warm-Sensitive Neurons that Control Body Temperature. Cell 167, 47–59.e15. [PubMed: 27616062]

Tasic B, Hippenmeyer S, Wang C, Gamboa M, Zong H, Chen-Tsai Y, and Luo L (2011). Site-specific integrase-mediated transgenesis in mice via pronuclear injection. Proc Natl Acad Sci U S A 108, 7902–7907. [PubMed: 21464299]

Ueno R, Narumiya S, Ogorochi T, Nakayama T, Ishikawa Y, and Hayaishi O (1982). Role of prostaglandin D2 in the hypothermia of rats caused by bacterial lipopolysaccharide. Proc Natl Acad Sci U S A 79, 6093–6097. [PubMed: 6964402]

Ushikubi F, Segi E, Sugimoto Y, Murata T, Matsuoka T, Kobayashi T, Hizaki H, Tuboi K, Katsuyama M, Ichikawa A, et al. (1998). Impaired febrile response in mice lacking the prostaglandin E receptor subtype EP3. Nature 395, 281–284. [PubMed: 9751056]

Woodward DF, Jones RL, and Narumiya S (2011). International Union of Basic and Clinical Pharmacology. LXXXIII: classification of prostanoid receptors, updating 15 years of progress. Pharmacol Rev 63, 471–538. [PubMed: 21752876]

Wu Z, Autry AE, Bergan JF, Watabe-Uchida M, and Dulac CG (2014). Galanin neurons in the medial preoptic area govern parental behaviour. Nature 509, 325–330. [PubMed: 24828191]

Yu S, Qualls-Creekmore E, Rezai-Zadeh K, Jiang Y, Berthoud HR, Morrison CD, Derbenev AV, Zsombok A, and Münzberg H (2016). Glutamatergic preoptic area neurons that express leptin receptors drive temperature-Dependent body weight homeostasis. J Neurosci 36, 5034–5046. [PubMed: 27147656]

Zhao ZD, Yang WZ, Gao C, Fu X, Zhang W, Zhou Q, Chen W, Ni X, Lin JK, Yang J, et al. (2017). A hypothalamic circuit that controls body temperature. Proc Natl Acad Sci U S A 114, 2042–2047. [PubMed: 28053227]

Highlights

- PGD_2 Synthase is a marker for temperature-sensitive neurons in preoptic area (POA).
- POA neurons that express PGD_2 Synthase are involved in thermoregulation.
- Rising POA temperature increases neuronal firing to promote PGD_2 production.
- PGD_2 activates DP1 receptor in ventral medial POA neurons that mediate hypothermia.

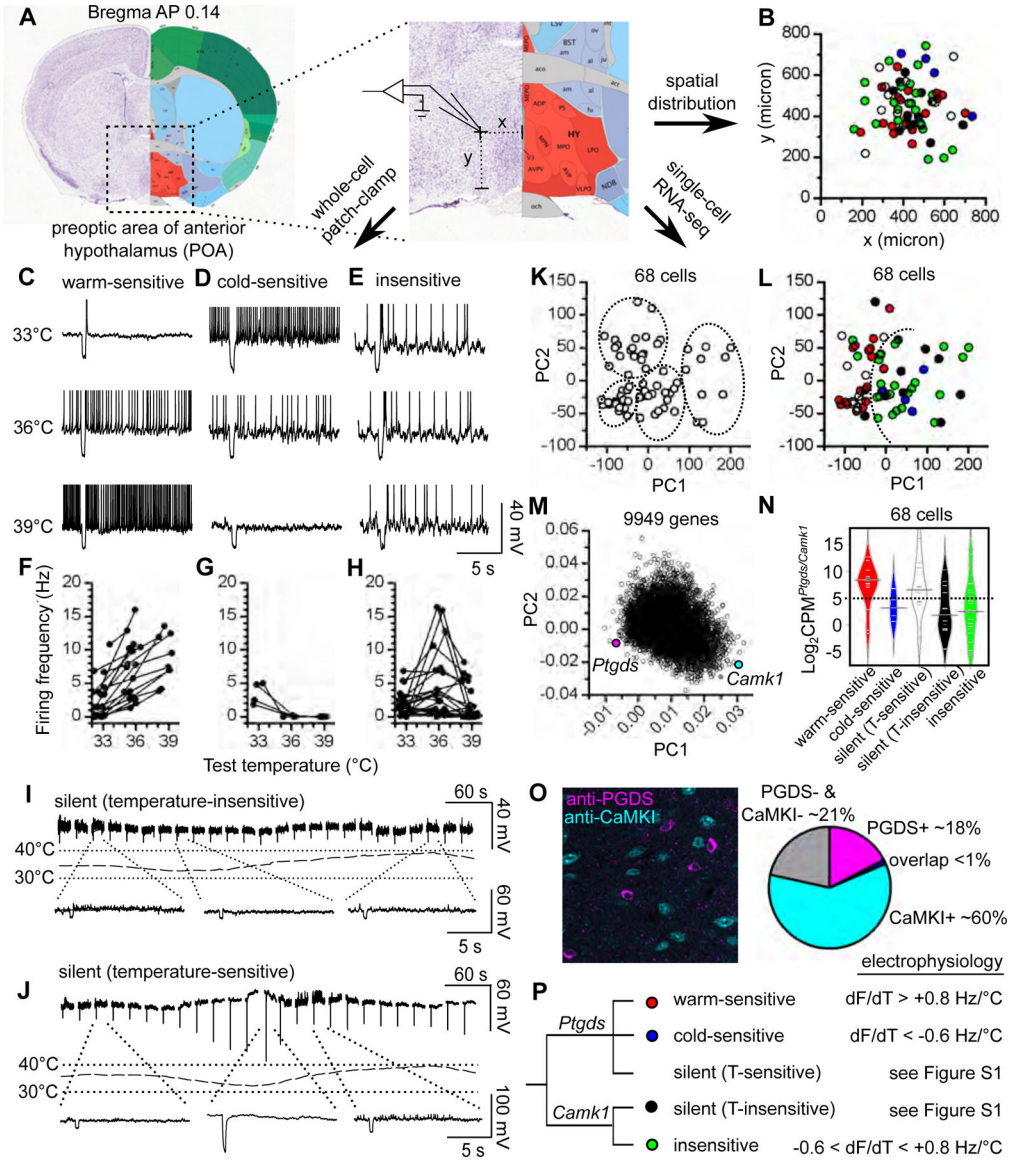

Figure 1. Genetic and functional profiling of neurons in mouse preoptic area (POA).

(A) Schematic illustration of the approach combining single-cell RNA-seq with whole-cell patch-clamp recording in POA slice; see also Figure S6B.

(B) Spatial distribution of analyzed neurons (N = 68) in POA, with color codes as in (**P**); x, horizontal distance to 3rd ventricle; y, vertical distance to optic chiasm.

(C-E) Sample current-clamp recordings of warm-sensitive neurons (**C**), cold-sensitive neurons (**D**), and temperature-insensitive neurons (**E**) at 33°C (top), 36°C (middle), and 39°C (bottom), with a −20 pA, 20 ms current pulse in each sweep to monitor membrane properties; action potentials truncated in display.

(F-H) The spontaneous action potentials (SAP) frequency at three different temperatures; (**F**) 18 warm-sensitive neurons, dF/dT > +0.8 Hz/°C; **(G)** 4 cold-sensitive neurons, dF/dT < −0.6 Hz/°C; **(H)** 24 temperature-insensitive neurons, −0.6 Hz/°C < dF/dT < 0.8 Hz/°C.

(I, J) Sample current-clamp recordings of temperature-insensitive silent neurons (**I**, $N = 12$) and temperature-sensitive silent neurons (**J**, $N = 10$); see also Figures S1.

(K, L) Principal component analysis (PCA) of the transcriptomes of 68 POA neurons, with K-means clustering (**K**, 4 groups, 5 replicates), or color labeling as in **(P)** to reflect their temperature sensitivity (**L**).

(M) Gene loadings from the PCA shown in **(K, L)**, with *Ptgds* and *Camk1* highlighted in magenta and cyan, respectively; see also Figure S3B.

(N) Expression ratio of *Ptgds* over *Camk1* in each neuron, quantified in log-scaled counts per million reads (Log_2CPM) from single-cell RNA-seq; short line, value of each individual neuron; long line, median value of each group.

(O) Antibody staining of L-PGDS (magenta, encoded by *Ptgds*) and CaMKI (cyan, encoded by *Camk1*) in mouse brain slices of POA (3 replicates, 264 cells); scale bar, 10 μm; blue, cells with both L-PGDS and CaMKI staining; grey, cells with neither L-PGDS nor CaMKI staining.

(P) Classification of POA neurons based on their gene expression and temperature sensitivity. See also Figure S2.

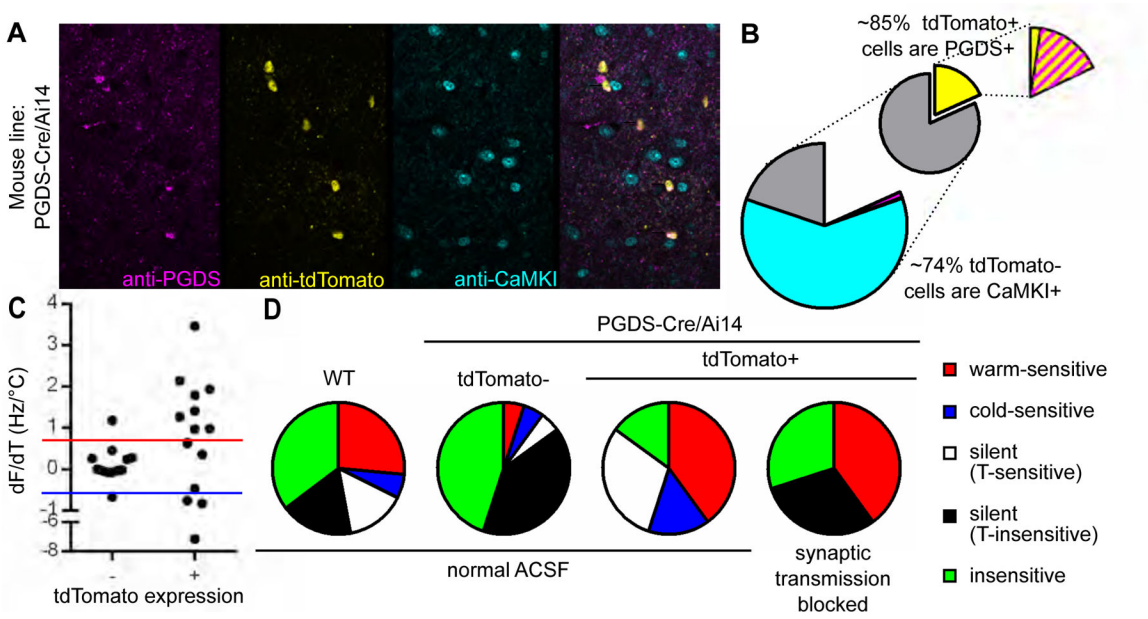

Figure 2. *Ptgds* is a genetic marker for temperature-sensitive POA neurons.

(A) Antibody staining of L-PGDS (magenta), tdTomato (yellow, labeling *Ptgds*-expressing cells), and CaMKI (cyan) in POA slices of PGDS-Cre/Ai14 mice (3 replicates); scale bar, 15 μm.

(B) ~85% neurons expressing tdTomato (yellow) have L-PGDS immunoreactivity (magenta); ~74% neurons without tdTomato expression (grey) have CaMKI immunoreactivity (cyan) (3 replicates, 459 cells); see also Figure S3C.

(C) Temperature sensitivity of POA neurons with (right) or without (left) *Ptgds*-expression marked with tdTomato; red and blue lines mark the criteria for warm-sensitive (dF/dT > +0.8 Hz/°C) and cold-sensitive (dF/dT < −0.6 Hz/°C) neurons, respectively; silent neurons were excluded from this plot.

(D) Temperature sensitivity of POA neurons from WT (WT/normal ACSF, $N = 68$) or PGDS-Cre/Ai14 mice, including neurons without *Ptgds* expression (tdTomato-/normal ACSF, $N = 20$; $P < 0.01$, Chi-square test, compared to WT), neurons with tdTomato marking *Ptgds* expression (tdTomato+/normal ACSF, $N = 20$; $P < 0.01$, Chi-square test, compared to WT), and PGDS-Cre/Ai14 mice with *Ptgds* expressing neurons recorded in the presence of synaptic transmission blockers (tdTomato+/synaptic transmission blocked, 20 μM DNQX, 50 μM AP5, and 20 μM SR 95531, $N = 20$; $P < 0.01$, Chi-square test, compared to tdTomato +/normal ACSF); color code as in Figure 1P.

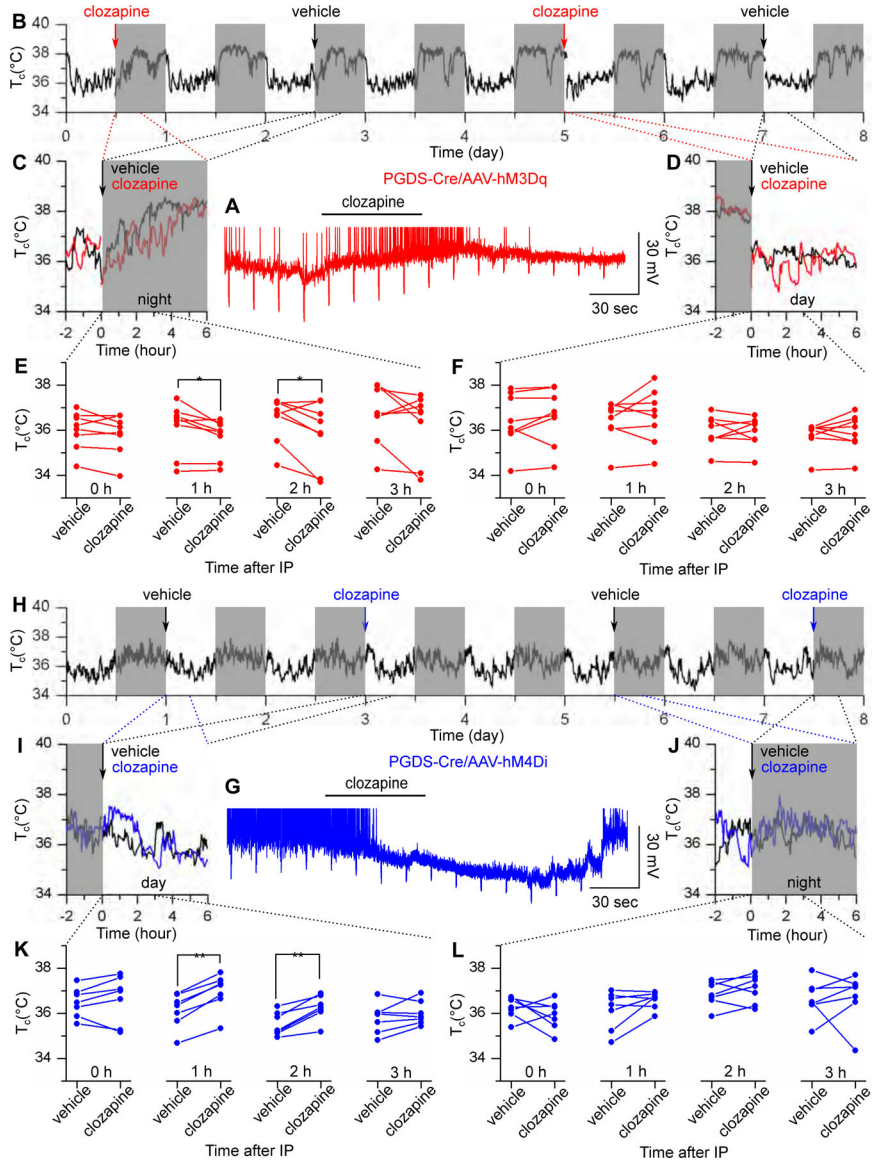

Figure 3. *Ptgds*-expressing POA neurons are involved in body temperature control.

(A, G) Sample current-clamp recordings of POA neurons expressing *Ptgds*-driven Cre and hM3Dq (**A**, red) or hM4Di (**G**, blue) (both labeled by mCherry) subjected to clozapine treatment (1 μ M, 1 min); action potentials truncated in display; see also Figure S4E.

(B, H) Sample core body temperature (T_C) recording (via an implanted probe) for > 8 days, from mice with hM3Dq **(B)** or hM4Di **(H)** in *Ptgds*-expressing POA neurons, with intraperitoneal (IP) injections of clozapine (10 μg/kg body weight) or vehicle, in early day- or night-time.

(C, D, I, J) Sample mouse T_C recording for 8 hours, with intraperitoneal (IP) injections of clozapine (red) or vehicle (black).

(E, F, K, L) Mouse T_C at 0–3 hours following IP. (N = 8 (hM3Dq) or 7 (hM4Di), **, P < 0.01, *, P < 0.05, paired Student's T-test). See also Figure S4.

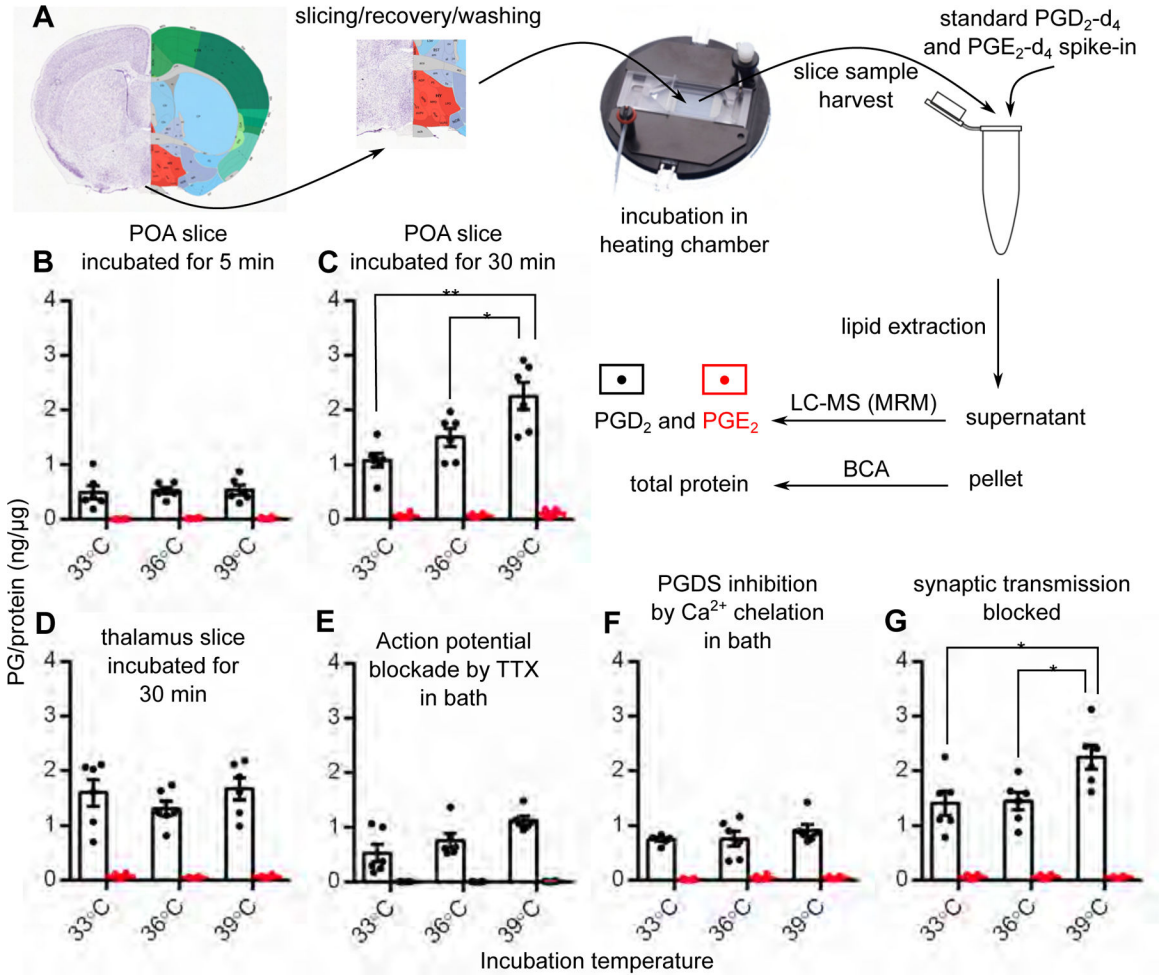

Figure 4. Prostaglandin D2 (PGD_2) production in POA is temperature-dependent.

(A) Schematic illustration of the approach using freshly prepared brain slices to analyze PGD_2 and PGE_2 production *in vitro*.

(B-G) PGD_2 (black) and PGE_2 (red) levels (normalized to total protein level) in brain slices of POA **(B, C, E, F, G)** or thalamus (**D**, with comparable amounts of protein input as POA samples), incubated at 33°C, 36°C, or 39°C, for 5 min **(B)** or 30 min **(C-G)**, in normal ACSF **(B-D)** or with treatments of TTX (1 μM, E), Ca^{2+} free ACSF (0 mM Ca^{2+}, 10 mM EGTA, **F)**, or synaptic transmission blockers (20 μM DNQX, 50 μ M AP5, and 20 μM SR 95531, **G)**; $N = 6$ in each condition; $P < 0.01$ in **C**, $P < 0.05$ in **G**, One-Way ANOVA; **, $P < 0.01$; *, $P < 0.05$, Tukey's multiple comparisons test; $P < 0.01$, One-Way ANOVA followed by Tukey's multiple comparisons test when comparing samples incubated in 36°C in **B, E, F** with **C**; mean ± s.e.m.

See also Figure S5.

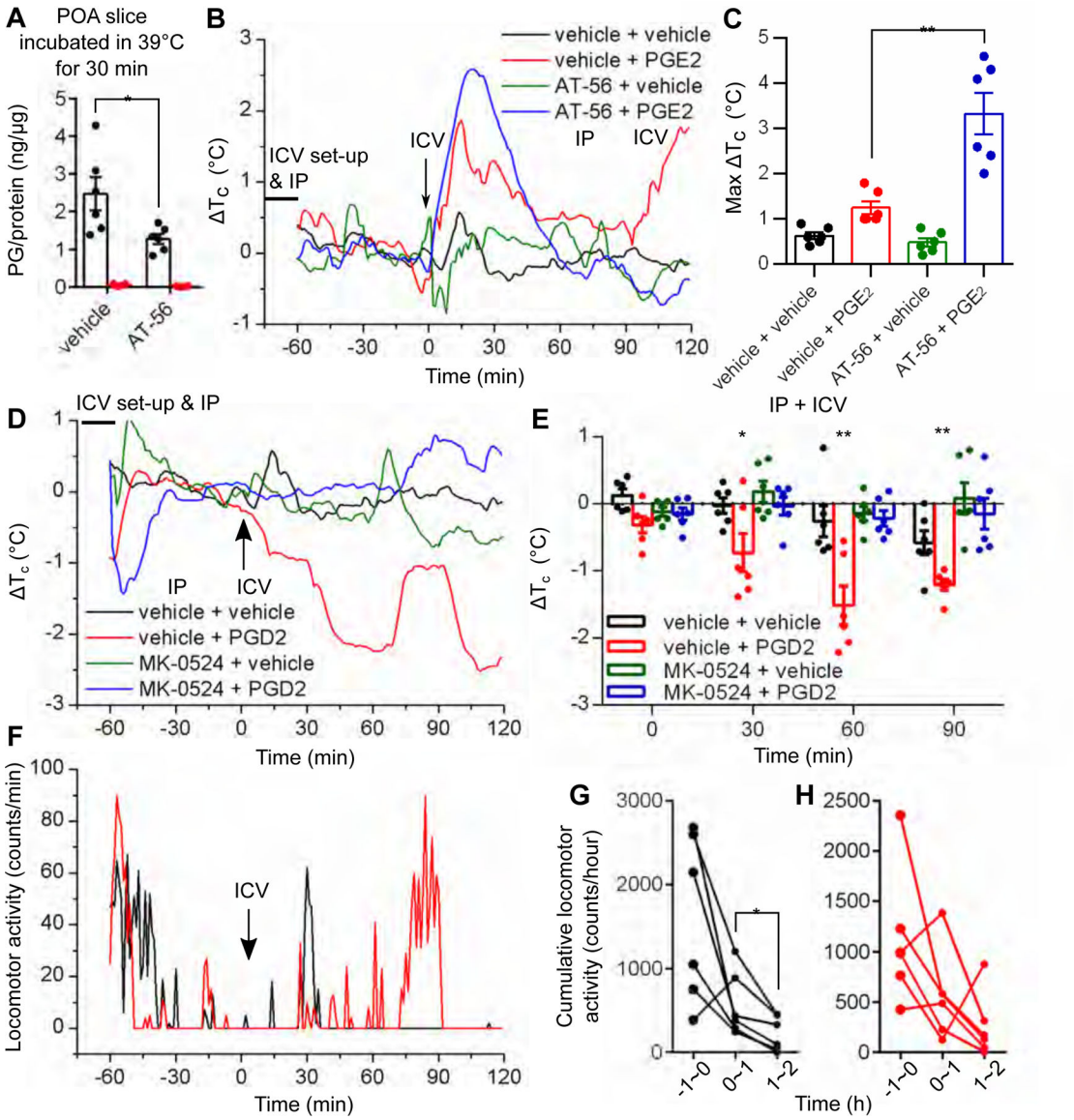

Figure 5. PGD_2 protects mouse from hyperthermia by mediating T_c decrease.

(A) PGD_2 (black) and PGE_2 (red) levels in POA slices incubated at 39°C for 30 min with L-PGDS inhibitor, AT-56 (20 μM), or vehicle ($N = 6$, *, $P < 0.05$, Student's T-test); mean ± s.e.m.

(B, C) IP injection of AT-56 (20 mg/kg body weight) induces higher body temperature increase (ΔT_c) in response to intracerebroventricular (ICV) injection of PGE_2 (2 nmol in 1μl); black, IP vehicle and ICV vehicle; red, IP vehicle and ICV PGE_2; green, IP AT-56 and ICV vehicle; blue, IP AT-56 and ICV PGE_2; $N = 6$ in each condition, $P < 0.01$, One-Way ANOVA, **, $P < 0.01$, Tukey's multiple comparison test; mean ± s.e.m.

(D, E) ICV injection of PGD_2 (2 nmol in 1 μl) into mouse lateral ventricle induces hypothermia, which can be abolished by prior IP injection of DP1 (PGD_2 receptor) blocker MK-0524 (4 mg/kg body weight); black, IP vehicle and ICV vehicle (same data set as in **B, C)**; red, IP vehicle and ICV PGD_2; green, IP MK-0524 and ICV vehicle; blue, IP MK-0524

and ICV PGD_2; *N* = 6 in each condition; **, P < 0.01, *, P < 0.05, One-Way ANOVA with repeated measurement, followed by Sidak's multiple comparisons test; mean ± s.e.m.
(F) Simultaneous recordings of T_c (D) and the locomotor activity (F) of mice, with ICV injection of PGD_2 (red) or vehicle (black), 3 hours following ICV set-up.
(G, H) The cumulative locomotor activity of mice in the 3 one-hour windows; *, P < 0.05, One-Way ANOVA with repeated measurement, followed by Sidak's multiple comparisons test.

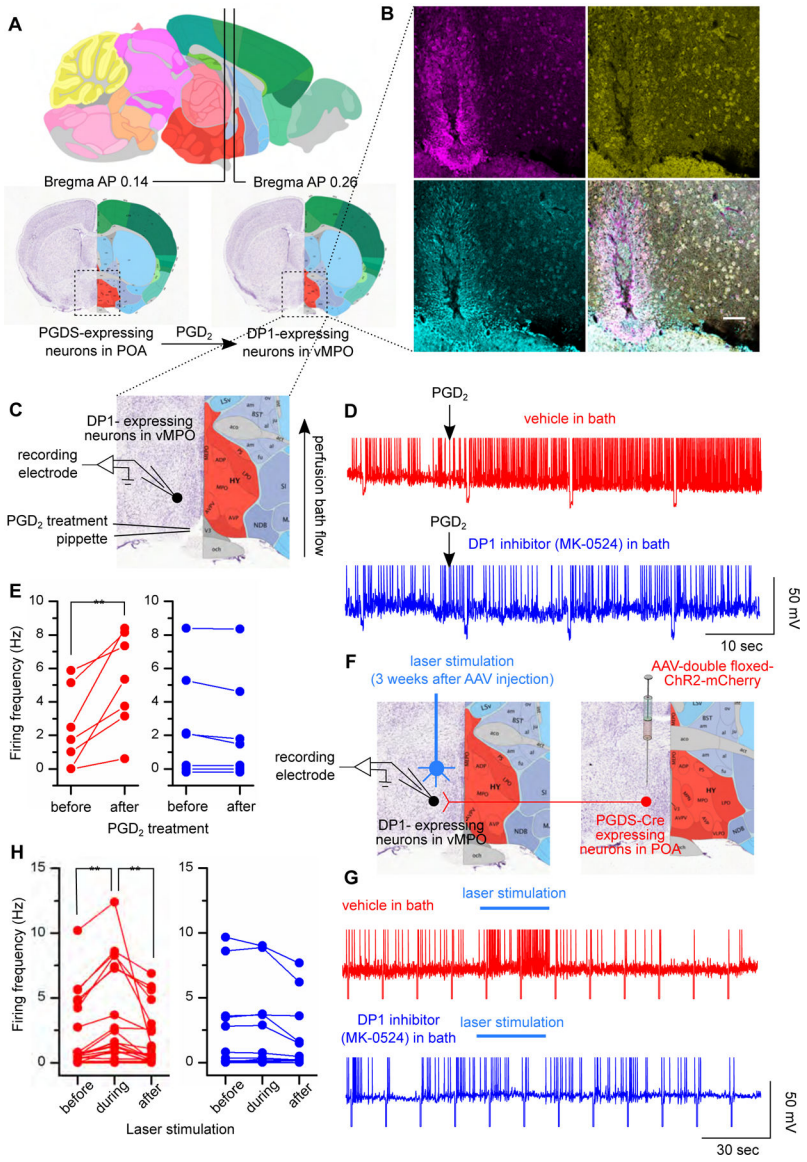

Figure 6. PGD_2 excites neurons in the ventral medial preoptic area (vMPO) by activating the PGD_2 receptor DP1.

(A) PGDS-expressing neurons in medial and lateral POA and DP1-expressing neurons in vMPO are in adjacent yet distinct brain regions; see also Figures S6A and S6B.

(B) The PGD_2 receptor DP1 (magenta) is expressed in vMPO neurons, co-localized with neural peptides BDNF (yellow) in putative soma and PACAP (cyan) in putative processes along the 3rd ventricle (3 replicates); scale bar, 50 μm; see also Figures S6C–S6F.

(C-E) Schematic illustration **(C)**, sample traces **(D)**, and summary **(E)** of current-clamp recordings from vMPO neurons in response to PGD_2 treatment (20 μM, ~10 s), in the presence of vehicle (red) or DP1 blocker MK-0524 (blue, 100 nM) ($N = 7$ in each condition; **, $P < 0.01$, paired Student's T-test); action potentials truncated in display.

(F-H) Schematic illustration **(F)**, sample traces **(G)** and summary **(H)** of current-clamp recordings from vMPO neurons in response to laser stimulation (~30 s), in the presence of vehicle (red, $N = 24$; **, $P < 0.01$, One-Way ANOVA with repeated measurement, followed

by Sidak's multiple comparisons test) or DP1 blocker MK-0524 (blue, 100 nM, $N = 18$; $P > 0.05$, One-Way ANOVA with repeated measurement); action potentials truncated in display. Recordings were carried out in the presence of 20 μM DNQX, 50 μM AP5, and 20 μM SR 95531; See also Figure S7.

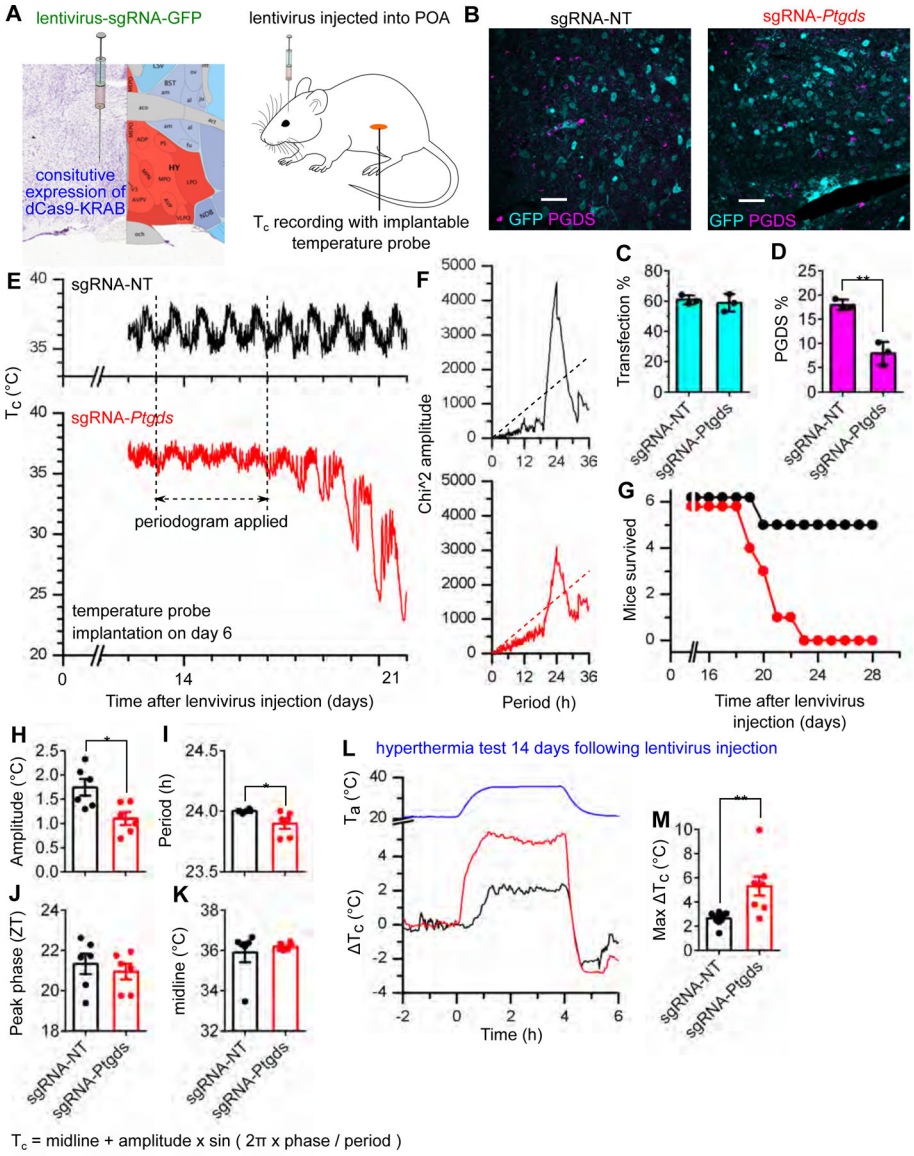

Figure 7. L-PGDS in POA temperature-sensitive neurons is crucial for thermoregulation and survival of animals.

(A) Schematic illustration of CRISPRi-mediated *Ptgds* knockdown in mouse POA.

(B) Antibody staining of GFP (cyan, marker for lentivirus transfection) and L-PGDS (magenta) in POA slices of dCas9-KRAB mice with sgRNA either non-targeting (NT) or targeting *Ptgds* (3 replicates in each condition); scale bar, 50 μm.

(C, D) Percentage of cells that are transfected with lentivirus (C, labeled with GFP) and percentage of cells that express L-PGDS (D) in medial and lateral POA of dCas9-KRAB mice with sgRNA of NT or *Ptgds*; $N = 3$ in each conditions, **, $P < 0.01$, Student's T-test); mean ± s.e.m.

(E, F) Sample mouse T_c recording following viral injection (E), with Chi-square periodogram of T_c oscillation in day 13–17 (F; dashed line, confidential interval of 0.001); black, sgRNA-NT; red, sgRNA-*Ptgds*.

(G) Survival rate of mice with viral injection of sgRNA-NT (black) or sgRNA-*Ptgds* (red); $N = 6$ in each condition; $P < 0.01$, log-rank test.

(H-K) Amplitude **(H)**, period **(I)**, peak phase **(J)**, and midline **(K)** of T_c oscillation of mice with viral injection of sgRNA-NT (black) or sgRNA-*Ptgds* (red), based on the periodogram of T_c recording in day 13–17; $N = 6$ in each condition; *, $P < 0.05$, Student's T-test; mean ± s.e.m.

(L, M) Sample traces **(L)** and summary **(M)** of T_c recordings of mice upon exposure to elevated ambient temperature (37°C, 4 hours) 2 weeks following lentivirus injection; black, sgRNA-NT, $N = 9$; red, sgRNA-*Ptgds*, $N = 8$; blue, ambient temperature; **, $P < 0.01$, Student's T-test.